arXiv:astro-ph/0512348v1 13 Dec 2005

Elemental Abundance Ratios in Stars of the Outer Galactic Disk. III. Cepheids[1]

David Yong

Department of Physics & Astronomy, University of North Carolina, Chapel Hill, NC 27599-3255; email: yong@physics.unc.edu

Bruce W. Carney

Department of Physics & Astronomy, University of North Carolina, Chapel Hill, NC 27599-3255; email: bruce@physics.unc.edu

Maria Luísa Teixera de Almeida

Department of Physics & Astronomy, University of North Carolina, Chapel Hill, NC 27599-3255; email: luisa@oal.ul.pt

Brian L. Pohl

Department of Physics & Astronomy, University of North Carolina, Chapel Hill, NC 27599-3255; email: bpohl@physics.unc.edu

ABSTRACT

We present metallicities, [Fe/H], and elemental abundance ratios, [X/Fe], for a sample of 24 Cepheids in the outer Galactic disk based on high-resolution echelle spectra. The sample have Galactocentric distances covering $12 \leq R_{\rm GC}$ (kpc) ≤ 17.2 making them the most distant Galactic Cepheids upon which detailed abundance analyses have been performed. We find sub-solar ratios of [Fe/H] and overabundances of [α/Fe], [La/Fe], and [Eu/Fe] in the program stars. All abundance ratios exhibit a dispersion that exceeds the measurement uncertainties. As seen in our previous studies of old open clusters and field giants, enhanced ratios of [α/Fe] and [Eu/Fe] reveal that recent star formation has taken place in the outer disk with Type II supernovae preferentially contributing ejecta to the ISM and with Type Ia supernovae playing only a minor role. The enhancements for La suggest that AGB stars have contributed to the chemical evolution of the outer Galactic disk.

Some of the young Cepheids are more metal-poor than the older open clusters and field stars at comparable Galactocentric distances. This demonstrates that

the outer disk is not the end result of the isolated evolution of an ensemble of gas and stars. We showed previously that the older open clusters and field stars reached a basement metallicity at about 10-11 kpc. The younger Cepheids reach the same metallicity but at larger Galactocentric distances, roughly 14 kpc. This suggests that the Galactic disk has been growing with time as predicted from numerical simulations.

The outer disk Cepheids appear to exhibit a bimodal distribution for [Fe/H] and [α/Fe]. Most of the Cepheids continue the trends with Galactocentric distance exhibited by Andrievsky's larger Cepheid sample and we refer to these stars as the "Galactic Cepheids". A minority of the Cepheids show considerably lower [Fe/H] and higher [α/Fe] and we refer to these stars as the "Merger Cepheids". One signature of a merger event would be composition differences between the "Galactic" and "Merger" Cepheids. The Cepheids satisfy this requirement and we speculate that the distinct compositions suggest that the "Merger Cepheids" may have formed under the influence of significant merger or accretion events. The short lifetimes of the Cepheids reveal that the merger event may be ongoing with the Monoceros ring and Canis Major galaxy being possible merger candidates.

Subject headings: Galaxy — disk; Clusters — abundances

1. INTRODUCTION

The Galactic disk accounts for the vast majority of stars in the Milky Way. Abundance analyses of nearby field stars (Edvardsson et al. 1993; Reddy et al. 2003), open clusters (Friel 1995), planetary nebulae (Henry et al. 2004), and H II regions (Shaver et al. 1983) have provided insight into the mean metallicity and metallicity gradient of younger and older stars and stellar remnants. Radial abundance gradients, as measured in disk stars, provide crucial constraints for models of the formation and evolution of our Galaxy (Hou et al. 2000; Chiappini et al. 2001). However, to explore the origin and continuing evolution of the Galactic disk, we need much more information than mean metallicities alone can

[1]This paper makes use of observations obtained at the National Optical Astronomy Observatory, which is operated by AURA, Inc., under contract from the National Science Foundation. We also employ data products from the Two Micron All Sky Survey, which is a joint project of the University of Massachusetts and the Infrared Processing and Analysis Center/California Institute of Technology, funded by the National Aeronautics and Space Administration and the National Science Foundation

provide. We need detailed elemental abundance ratios, which contain vital information on the relative contributions of Type II supernovae, Type Ia supernovae, and asymptotic giant branch (AGB) stars.

In order to address this situation, we commenced an observing program to measure metallicities and detailed chemical compositions for stars in the outer Galactic disk. An analysis of the radial velocities and chemical abundance patterns of four old open clusters with Galactocentric distances between 12 and 23 kpc was presented in Paper I (Yong et al. 2005). In Paper II (Carney et al. 2005), we continued our attack upon the outer disk by initiating a successful selection process for identifying distant field giants then conducting an abundance analysis of three such stars. From these analyses, two principal findings may be noted: (1) at large Galactocentric distances, $R_{\rm GC} > 10$ kpc, the expected metallicity gradient vanishes and the stars exhibit a constant value of [Fe/H] ≈ -0.5; (2) field and cluster stars in the outer Galactic disk show enhancements for the "α" elements, [α/Fe] $\approx$ 0.2. Our interpretation was that these abundance patterns reflected the episodic growth of the disk via accretion or merger events. These events triggered rapid star formation with Type II supernovae preferentially contributing to the chemical enrichment.

The open clusters are old, with ages between 2 - 6 Gyr. The ages of the field giants are unknown, but presumably these stars are quite old too. The absence of the radial abundance gradient inferred from our sample of distant field and clusters stars may therefore not reflect the current situation in the outer disk. The time variation of the Galactic radial abundance gradient offers a more comprehensive test of Galactic evolution models than a single epoch (or time integrated) abundance gradient. The possibility of an on-going merger event in the outer disk (e.g. Newberg et al. 2002; Ibata et al. 2003; Yanny et al. 2003; Martin et al. 2004) reinforces the need to analyze a sample of young stars at large distances and to measure detailed abundance ratios [X/Fe] in addition to the metallicity, [Fe/H].

Cepheids are high-mass stars whose short lifetimes ensure that their atmospheres reflect the present-day composition of the ISM. Abundance analyses of Cepheids appear feasible (Fry & Carney 1997; Andrievsky et al. 2002a,b,c, 2004; Luck et al. 2003) and the Cepheid period-luminosity relation allows for accurate distance determinations. Due to their luminosity, high-resolution spectroscopic observations of Cepheids located at large distances can be conducted with modest-sized telescopes. In this paper, the third of this series, we present metallicities, [Fe/H], and elemental abundance ratios, [X/Fe], for a sample of two dozen Cepheids with Galactocentric distances $12 \leq R_{\rm GC} \leq 17.2$ kpc. These Cepheids allow us to study the Galactic radial abundance gradient as a function of time. Detailed abundance ratios [X/Fe] offer an insight into the events currently taking place in the outer disk and such abundance ratios may reveal the signatures of recent merger events.

2. PROGRAM STARS AND OBSERVATIONS

2.1. Target selection

We compiled a list of 421 Type I Cepheids using three primary sources: the Cepheid database maintained by Fernie at the University of Toronto[2], Caldwell & Coulson (1987), and Metzger et al. (1998). Periods were taken from the Fourth Edition of the General Catalog of Variable Stars[3]. Optical photometry and reddening estimates were obtained from these references, supplemented by reddening estimates of Fernie (1990). We then calculated heliocentric and Galactocentric distances for all these stars using the visual band period-luminosity relation of Madore & Freedman (1991). We identified a list of thirty Cepheids with Galactocentric distances $R_{\rm GC} > 12.5$ kpc of which 10 had $R_{\rm GC} > 14$ kpc. Spectra for all 10 Cepheids with $R_{\rm GC} > 14$ kpc and 14 of the 20 with $12.5 < R_{\rm GC} < 14.0$ kpc were obtained during a series of observing runs (see Table 1).

2.2. Observations and data reduction

The targets were observed using the echelle spectrographs on the 4-meter telescopes at the Kitt Peak National Observatory (KPNO) and the Cerro Tololo Inter-American Observatory (CTIO) during four different observing runs between 1997 December and 1999 January. Red long red cameras were used with the 31.6 lines mm^{-1} echelle gratings. Second-order blue light was blocked using GG495 filters. The wavelength coverage was 5500-8000Å at CTIO and 4700-8000 Å at KPNO with the difference resulting from the choice of cross-dispersers, G181 at CTIO (316 lines mm^{-1}) and G226 at KPNO (226 lines mm^{-1}). A 1.0″ slit (150 microns) provided a spectral resolution of 28,000 (two pixels per resolution element) and a dispersion of 0.07 pixel at 5800Å. Generally we were able to achieve signal-to-noise ratios (S/N) of about 75 per pixel (108 per resolution element).

The observing routine included 20 quartz lamp exposures to provide data for flat-fielding, and 15 zero-second exposures to provide "bias" frames. Th-Ar hollow cathode lamp spectra were taken before and after each stellar exposure. The data were reduced using the IRAF[4] packages IMRED, CCDRED, and ECHELLE to correct for the bias level,

[2]www.astro.utoronto.ca/DDO/research/cepheids/cepheids.html

[3]www.mai.sai.su/groups/cluster/gcvs/gcvs

[4]IRAF (Image Reduction and Analysis Facility) is distributed by the National Optical Astronomy Observatory, which is operated by the Association of Universities for Research in Astronomy, Inc., under contract

trim the overscan region, extract individual orders, fit the continuum, apply a wavelength solution using the Th-Ar spectra. Master flat field frames were produced each night, and normalized using APFLATTEN, following which the data frames were divided by the master flat field frames prior to extraction of individual orders using APALL. The wavelength solution was determined from Th-Ar comparison spectra obtained after each program star. ECIDENTIFY and DISPCOR were used to identify the Th-Ar lines and determine the dispersion solution for each order, and the CONTINUUM task enabled us to interactively fit a high-order cubic spline to produce the continuum-normalized, wavelength-calibrated spectra. Stars with more than one observed spectrum were cross-correlated and then combined into a single final spectrum using SCOMBINE. (The spectra were only combined if they were obtained sufficiently close in time to ensure that the phases were essentially identical.) In Figures 1 and 2, we show the final reduced spectra for two pairs of Cepheids. As we describe below, we believe that the two Cepheids in Figures 1 and 2 have nearly identical effective temperatures ($\approx$ 5625K in Figure 1 and $\approx$ 6400K in Figure 2). Figure 2 clearly shows that there is a significant spread in chemical abundances among Cepheids in the outer Galactic disk.

2.3. Overtone pulsators

Most Cepheids pulsate in the fundamental mode, and the period-luminosity relation applies only to such stars. Nonetheless, we must be careful to try to verify the pulsational mode of our program stars so that we may reliably calculate their distances.

First overtone pulsators are more common among the shorter period stars. For stars with metallicities similar to what are expected in the outer Galactic disk, and which we obtain for our program stars, an excellent reference is the very extensive work by Alcock et al. (1995) on Cepheid variables in the Large Magellanic Cloud. Their Figure 5 shows clearly the offset in the V vs. log P relation that identifies the overtone pulsators. It is clear that at the metallicity of the LMC, [Fe/H] ≈ -0.3, the stars with periods shorter than about 2.5 days have a reasonably high probability of pulsating in the first overtone mode.

We have relied upon the on-line version of the General Catalog of Variable Stars to help identify the first overtone pulsators in our sample, which may generally be identified by the more sinusoidal, more symmetric shape of the optical light curves. NY Cas is pulsating in the first overtone, but we note that Table 1 reveals that three other stars, EW Aur, GP Per, and XZ CMa, have pulsational periods of less than 3 days. We have corrected the observed

---

with the National Science Foundation.

pulsation period of NY Cas to its equivalent fundamental mode, 4.01 days, using the relation provided by Alcock et al. (1995). We have not adjusted the distance estimates for the other three stars, but caution the reader that these distances may be underestimated.

2.4. Distance estimations

Distances to Cepheids are readily obtained from the period-luminosity relation. Our program stars were selected to lie at large Galactocentric distances and are located in the Galactic plane. Therefore the effects of interstellar reddening and extinction are important and must be taken into account. At longer wavelengths, extinction and reddening are less significant such that $A_K = 0.11 A_V$. Therefore, we rely on infrared photometry from 2MASS to determine the distances to the program Cepheids. We employ the relation from Madore & Freedman (1991)

$$M_{K(\mathrm{CIT})} = -3.42(\log P - 1.00) - 5.70 \quad (1)$$

after converting the magnitudes from the 2MASS system to the CIT system via the transformations provided by Carpenter (2001). We also converted the single epoch 2MASS K magnitudes to mean K magnitudes according to the prescription given by Soszynski et al. (2005). In Figure 3 we compare our adopted reddenings with those derived from the Schlegel et al. (1998) dust maps. As expected, the adopted reddenings are all equal to or less than the Schlegel et al. (1998) values. Our program Cepheids are located at Galactocentric distances $12.0 \leq R_{\mathrm{GC}}(\mathrm{kpc}) \leq 17.2$. Seven of our Cepheids, CE Pup, EE Mon, ER Aur, FO Cas, HQ Car, IO Cas, and NY Cas, lie at Galactocentric distances beyond $R_{\mathrm{GC}} = 15$ kpc and are the most distant Galactic Cepheids whose chemical compositions have been analyzed.

We assert that the largest uncertainty in our distance estimation is due to the conversion from single epoch 2MASS K magnitudes to mean K magnitudes. Soszynski et al. (2005) estimate that the uncertainties in mean K magnitude for Galactic Cepheids are about 0.03 mag which corresponds to distance errors of 0.2 kpc. A 0.1 mag error in E$(B-V)$ also corresponds to a distance error of 0.2 kpc. Perhaps the most direct test of the uncertainties in our distances is to compare the values derived from V and from K. The mean difference is distance (K) − distance (V) = 0.23 kpc (σ = 0.72). Therefore we take 0.7 kpc as a representative uncertainty in our Cepheid distances.

3. ELEMENTAL ABUNDANCES

3.1. Stellar parameters

The effective temperature ($T_{\rm eff}$), surface gravity ($\log g$), and microturbulent velocity (ξ_t) were determined using spectroscopic criteria. This is the same method that was used in Paper I and Paper II as well as by Fry & Carney (1997) who undertook an analysis of nearby Cepheids that calibrate the period-luminosity relation. Equivalent widths were measured for a set of Fe I and Fe II lines using routines in IRAF. The gf-values for the Fe I lines were taken from the laboratory measurements performed by the Oxford group (e.g., Blackwell et al. 1979a,b, 1980, 1986a, 1995 and references therein). For Fe II lines, we used the gf-values from Biémont et al. (1991). The full list of Fe I and Fe II lines are presented in Table 2. Local thermodynamic equilibrium (LTE) model atmospheres were computed using the ATLAS9 program (Kurucz 1993) and we used the LTE stellar line analysis program MOOG (Sneden 1973). We set $T_{\rm eff}$ by forcing the abundances from Fe I lines to be independent of the lower excitation potential. We adjusted $\log g$ until the abundances from Fe I and Fe II agreed. Finally, the microturbulence was determined by insisting that the abundances from Fe I lines show no trend versus EW. This process required iteration until a self-consistent set of parameters was obtained. In Papers I and II we employed an identical procedure for determining the stellar parameters of the older cluster and field red giants. In Section 3.5 below we consider more carefully whether our approach is appropriate. The stellar parameters presented in Table 3 are those adopted for the subsequent abundance analysis.

3.2. Elemental abundance analysis

Next we measured EWs for lines of the α elements Mg, Si, Ca and Ti again using routines in IRAF. Abundances were determined via MOOG based on the measured EW, model atmosphere, and atomic data. The gf-values for Ca and Ti were taken from the Oxford group (Smith & Raggett 1981; Blackwell et al. 1982, 1983, 1986b). For Si, an inverted solar analysis assuming $\log \epsilon({\rm Si}) = 7.55$ was used to determine the gf-values. For Mg, we relied upon the gf-values employed by Ramírez & Cohen (2002). For lines of the s-process element La, we took the gf-values from Lawler et al. (2001a) and included the effects of hyperfine splitting. For the r-process element Eu, the gf-values were taken from Lawler et al. (2001b) and take into account hyperfine and isotopic splitting (we assumed a solar isotopic mix). To measure the Eu abundance, we performed spectrum synthesis. The full list of atomic lines is presented in Table 2 and the adopted solar abundances were presented in Paper I. Recall that in Paper I our line lists and analysis procedures successfully reproduced the abundance

distributions in the Sun, Arcturus, and three stars close to the tip of the red giant branch in the old open cluster M67. We present the abundance ratios for the program Cepheids in Table 4. Typical internal errors for our spectroscopic model parameters are $T_{\rm eff}$ ± 150K, $\log g$ ± 0.3 dex, and ξ_t ± 0.3 km s^{-1}. In Table 5 we present the abundance dependences upon the model parameters.

3.3. Comparison with Fry & Carney

While the program stars are outer disk Cepheids, our overall goal is to compare the young stars in the inner and outer Galactic disk. In order to compare the compositions of the outer disk Cepheids with their solar neighborhood counterparts, we re-analyzed a subset of the Fry & Carney (1997) sample that included Cepheids with $6 \leq R_{\rm GC} \leq 10$ kpc. The principal differences between these two analyses are the adopted gf-values for Fe as well as the selection of Fe lines. The first simple test performed concerns the measurement of EWs in identical spectra. For U Sgr at two different phases, we measured EWs for the lines analyzed by Fry & Carney. In Figure 4, we compare the measured EWs. For the 75 common lines, the mean difference for THIS STUDY − FRY & CARNEY is −1.6 ± 0.5 (σ = 4.6 mÅ). Such a comparison demonstrates that the measured EWs cannot be responsible for any systematic differences that may arise between the two studies. Next we consider the gf-values used by the two studies. In Figure 5, we compare the adopted gf-values for the lines common to both studies. The scatter for Fe I lines is considerable, especially for lines with lower excitation potentials between 2 and 5 eV with the maximum discrepancy reaching 0.3 dex. Not all lines are measurable in every Cepheid. Therefore, depending on the set of measured lines, we anticipate possible differences in $T_{\rm eff}$ between the two studies resulting from the adopted Fe I gf-values. We may also expect some differences in microturbulent velocities. The gf-values for Fe II lines are in good agreement with the maximum difference being about 0.15 dex. Depending on the selection of measured Fe II lines, there may be small differences in the derived surface gravity.

For the comparison sample of local Cepheids, we utilize the identical spectra obtained and analyzed by Fry & Carney. Recall that Fry & Carney applied the same spectroscopic criteria that we have imposed when setting their stellar parameters. In Table 6 we show our stellar parameters and abundance ratios for a sample of solar neighborhood Cepheids. In total there are 11 Cepheids observed at 19 phases in common between the two studies. In Figure 6 we plot the differences in stellar parameters $\Delta T_{\rm eff}$, $\Delta \log g$, and $\Delta \xi_t$ versus $T_{\rm eff}$ (this study). The mean offsets are $\Delta T_{\rm eff}$ = −1 ± 23 (σ = 100 K), $\Delta \log g$ = −0.33 ± 0.05 (σ = 0.22 cgs), and $\Delta \xi_t$ = 0.18 ± 0.10 (σ = 0.45 km s^{-1}). The quoted differences are for

THIS STUDY − FRY & CARNEY. An interesting feature is that there appears to be a trend between $\Delta T_{\rm eff}$ and $T_{\rm eff}$ (this study). This may be related to the difference in gf-values between the two studies. Another possibility is that lines with systematically or randomly different gf values at lower and higher excitation potentials are being used. Our gravities are systematically lower than those obtained by Fry & Carney. In this case, there doesn't appear to be a trend with $T_{\rm eff}$. The difference in $\log g$ may also be a result of line selection and the corresponding gf-values. For the microturbulence, there is one obvious outlier. If we remove this outlier, there does not appear to be a trend between $\Delta\xi_t$ and $T_{\rm eff}$. For all stellar parameters, we emphasize that the mean offsets and dispersions are comparable to the internal uncertainties of this study.

For the purposes of this study, the crucial offsets we seek to measure are for the abundance ratios [Fe/H] and [X/Fe]. In Figure 7, we plot the abundance differences Δ[Fe/H] and Δ[X/Fe] for THIS STUDY − FRY & CARNEY versus $T_{\rm eff}$ (this study). The mean offsets are Δ[Fe/H] = -0.11 ± 0.02 ($\sigma = 0.08$), Δ[Si/Fe] = 0.03 ± 0.02 ($\sigma = 0.07$), Δ[Ca/Fe] = -0.04 ± 0.02 ($\sigma = 0.07$), Δ[Ti I/Fe] = -0.13 ± 0.02 ($\sigma = 0.10$), Δ[Ti II/Fe] = -0.08 ± 0.03 ($\sigma = 0.13$), and $\Delta[\alpha/{\rm Fe}] = -0.06 \pm 0.01$ ($\sigma = 0.05$).

The first point we draw attention to is that we confirm the Fry & Carney conclusion that self-consistent results can be obtained from a traditional spectroscopic analysis. For 8 Cepheids, we analyzed the spectra obtained at two different phases and found that [Fe/H] and [X/Fe] are essentially identical (see columns 6-14 of Table 6). In some cases, the constancy of the measured compositions prevails despite a change of 1000 K in a star's effective temperature.

An interesting feature of the abundance comparison is that there appears to be a trend between Δ[Fe/H] and $T_{\rm eff}$ (this study). As $T_{\rm eff}$ decreases, the magnitude of the offset between the iron abundances increases with the maximum discrepancy reaching -0.25 dex at $T_{\rm eff}$ = 5000 K. This is unsurprising given that $\Delta T_{\rm eff}$ showed a trend with $T_{\rm eff}$ (this study) and in Table 5, the Fe abundance based on Fe I lines is rather sensitive to $T_{\rm eff}$. Again, we suggest that this trend may be due to line selection and the corresponding gf-values. While a more detailed investigation is beyond the scope of the current paper, clearly the trend between $\Delta T_{\rm eff}$ and $T_{\rm eff}$ as well as the trend between Δ[Fe/H] versus $T_{\rm eff}$ warrant further attention. We intend to re-analyze the entire Fry & Carney sample. Though we have confirmed that self-consistency in the measured compositions can be obtained at two different phases using traditional spectroscopic techniques, a re-analysis over the entire pulsation cycle is of great interest.

Despite the trend between Δ[Fe/H] and $T_{\rm eff}$ (this study), for all other abundance ratios [X/Fe], we find no obvious trends between Δ[X/Fe] versus $T_{\rm eff}$. Inspection of Table 5,

reveals that the mean offsets for [X/Fe] between these two analyses are comparable to the uncertainties in the model parameters.

3.4. Comparison with Andrievsky

The Cepheids listed in Table 6 were also studied in the series of papers by Andrievsky and collaborators (Andrievsky et al. 2002a,b,c; Luck et al. 2003; Andrievsky et al. 2004). In addition to these nearby Cepheids, four outer disk Cepheids CU Mon, EE Mon, HW Pup, and WW Mon were also analyzed by Andrievsky. In total there are 15 Cepheids observed at 23 phases in common between these studies and ours.

Andrievsky's analysis differs from this study and from Fry & Carney (1997) in several ways. First, their gf-values were obtained using an inverted solar analysis. Second, the $T_{\rm eff}$ scale was set using line depth ratios. Third, microturbulent velocities were obtained from Fe II lines only, not Fe I lines. Finally, while the gravity was set via ionization equilibrium, the adopted Fe I abundance was not the mean abundance based on all Fe I lines. Instead, the Fe I abundance was inferred by plotting the abundance versus EW for all Fe I lines then extrapolating to an EW of 0 mÅ.

While there are 15 Cepheids in common, none were observed at identical phases. Therefore we cannot directly compare the stellar parameters between the two studies. However, we can compare the derived abundance ratios [Fe/H] and [X/Fe]. In Figure 8 we plot the abundance differences Δ[Fe/H] and Δ[X/Fe] for THIS STUDY − ANDRIEVSKY versus $T_{\rm eff}$ (this study). The mean offsets are Δ[Fe/H] = -0.16 ± 0.02 ($\sigma = 0.09$), Δ[Mg/Fe] = 0.23 ± 0.03 ($\sigma = 0.13$), Δ[Si/Fe] = 0.13 ± 0.02 ($\sigma = 0.09$), Δ[Ca/Fe] = 0.08 ± 0.01 ($\sigma = 0.06$), Δ[Ti/Fe] = 0.02 ± 0.02 ($\sigma = 0.10$), $\Delta[\alpha$/Fe] = 0.11 ± 0.01 ($\sigma = 0.04$), Δ[La/Fe] = 0.12 ± 0.02 ($\sigma = 0.10$), and Δ[Eu/Fe] = 0.19 ± 0.02 ($\sigma = 0.10$).

We again find a trend between Δ[Fe/H] and $T_{\rm eff}$ as seen in the comparison with Fry & Carney. Specifically, the magnitude of the offset between iron abundances increases as $T_{\rm eff}$ decreases with the maximum discrepancy reaching about -0.3 dex at $T_{\rm eff}$=5000 K. We believe this trend is due to the adoption by Andrievsky of the Fry & Carney (1997) effective temperatures to calibrate the line depth ratios versus $T_{\rm eff}$ relation.

There are no obvious trends between Δ[X/Fe] and $T_{\rm eff}$, despite the trend between Δ[Fe/H] and $T_{\rm eff}$. This was also seen in the comparison with Fry & Carney suggesting that abundance ratios may be measured reliably. Again, we note that in many cases, the mean offsets for [X/Fe] are comparable to the values arising from the uncertainties in the stellar parameters (see Table 5). In the subsequent sections, we apply these offsets to the

Andrievsky Cepheid abundances when investigating the radial abundance gradient.

3.5. Validity of a traditional spectroscopic approach

Andrievsky chose a non-standard approach as described above (see Kovtyukh & Andrievsky 1999 and Kovtyukh & Gorlova 2000 for a more detailed discussion). The fundamental reason for adopting a non-standard analysis was to avoid non-LTE effects. Fe I lines are more susceptible than Fe II lines to non-LTE effects due to the ionization balance in F and G stars. That is, most of the Fe is in the form of Fe II with Fe I being the minor species at these temperatures. Overionization of Fe atoms (relative to LTE) may result from the penetration by ultraviolet photons into the line-forming regions and such an effect would be lessened for the dominant species but may be serious for the minor component. In F and G stars, the effect of overionization would be an underabundance of Fe I in LTE analyses. As the dominant species, Fe II would only be slightly affected and may show a small overabundance. Were this a large effect, it would compromise the $T_{\rm eff}$ scale based on excitation equilibrium of Fe I, the surface gravities based on ionization equilibrium of Fe, and the microturbulent velocities set from Fe I lines.

Andrievsky's concerns regarding the reliability of the abundance analysis of Cepheids led to a non-traditional approach for the determination of the stellar parameters. While this method has merit, we do have some concerns. We have noted that the temperatures used in Andrievsky's initial calibration of the line depth ratios were taken from the Fry & Carney $T_{\rm eff}$ scale. Recall that the Fry & Carney temperatures were derived using excitation equilibrium of Fe I lines. Therefore, the very problem Andrievsky wished to avoid (i.e., possible non-LTE effects on Fe I lines) was the underlying assumption that provided the effective temperatures for their initial calibration. Additionally, a given line depth ratio becomes increasingly uncertain as the S/N decreases. For the most distant Cepheids, Andrievsky et al. were working with S/N ratios as low as 40 from which accurate $T_{\rm eff}$ must be very difficult to measure from line depth ratios.

If non-LTE effects of Fe I lines are significant, then using Fe II lines to derive the microturbulence would appear to be a better method. However, for some program Cepheids, the small number of Fe II lines (e.g., N $<$ 10) may lead to less accurate values of ξ_t.

Luck & Lambert (1985) recognized that the spectroscopically-determined gravity may systematically differ from the physical gravity in intermediate-mass supergiants. A deficiency in the measured O abundances in Cepheids was noted and Luck & Lambert (1985) showed that the O abundance was correlated with the difference between physical and spectroscopic

gravities. This correlation was interpreted as a possible consequence of systematic errors in the analysis. An alternative explanation offered was that the O underabundance was already present in the interstellar gas out of which the stars formed. Andrievsky et al. found that the spectroscopic gravity can be made to match the physical gravity if the Fe I abundance is estimated by extrapolating to an EW of 0 mÅ. In combination with their $T_{\rm eff}$ and microturbulent velocities, Andrievsky's gravity scale removed the O underabundance.

In Figure 9 we plot the spectroscopically determined gravities versus pulsational period and overplot the period-gravity relation for variable stars defined by Fernie (1995). For the longer period Cepheids, the spectroscopic gravities tend to be lower than the physical gravities. In general, the spectroscopic gravities tend to scatter about the period-gravity relation. For our programs Cepheids and the subset of the Fry & Carney (1997) sample that we re-analyzed, we find a mean difference $\Delta \log\ g = \log g_{\rm spec} - \log g_{\rm period} = -0.19 \pm 0.07$ ($\sigma = 0.48$). The scatter is considerably larger than our estimated internal error of about 0.3 dex, and the similar amount of scatter in the comparison with the results from Fry & Carney (1997). We attribute the 0.5 dex scatter to three causes, in addition to our internal uncertainties. First, of course, the actual $\log\ g$ vs. $\log\ P$ relation must have scatter. Unfortunately, the Cepheid portion of the relation was defined using models rather than observations, so this source of error cannot be quantified. Second, the distribution does not appear to follow a simple Gaussian distribution. Three stars (IO Cas, YZ Aur, and OT Per) depart significantly from the relation. Excluding these three stars lowers the scatter in the predicted vs. derived $\log g$ values to only 0.40 dex, which is probably consistent with the convolution of our uncertainties and those in the relation of Fernie (1995). Third, there is the question of non-LTE effects noted above. Qualitatively, we would expect the longer period stars, with the lowest gravities, to be affected most. Indeed, two of the three stars with the largest deviations have long periods, YZ Aur (18.2 days) and OT Per (26.1 days). Other stars with comparably long periods, however, appear to provide an excellent match to the relation. Because of the importance of the non-LTE issue, we explore this further.

We begin by considering the behavior of four of our key derived quantities vs. the logarithm of the pulsation period (see Figure 10). We distinguish between stars from the outer disk in this program, shown as filled circles, from those of the local disk, from Fry & Carney (1997) and re-analyzed by us (see Table 6), shown as crosses. The top panel shows that the temperatures derived for the two samples share the same behavior as a function of period, and consistent with the longer period, lower gravity stars in the instability strip also being cooler. The second panel shows that the local cepheids show very similar [Fe/H] values, independent of period (and therefore gravity), while the outer disk cepheids are more metal-poor. This foreshadows the following discussion, but is certainly expected in the Galaxy due to an anticipated gradient in mean metallicity as a function of Galactocentric distance.

The third panel of Figure 10 concentrates on possible trends in element-to-iron ratios. We select calcium for the comparison because the [Ca/Fe] values are well determined, and because its ionization potential is the lowest of the four elements that define our measurable "α" elements (Mg, 7.65 eV; Ca, 6.11 eV; Si, 8.15 eV; and Ti, 6.82 eV). If non-LTE effects are important, they should be more pronounced for elements with lower ionization potentials, and hence we might discover a trend in [Ca/Fe], since the ionization potential for iron is much higher, 7.90 eV. The Figure shows no such trend, although it again foreshadows our results: the outer disk Cepheids show enhanced [Ca/Fe] values compared to local Cepheids.

The bottom panel of Figure 10 carries the non-LTE test further, where we compare the differences of [Ti/Fe] derived from lines of Ti I and Ti II. For the program Cepheids, we find a mean difference [Ti I/Fe] − [Ti II/Fe] = 0.07 ± 0.02 ($\sigma = 0.11$). This difference lies within the measurement uncertainties suggesting that the surface gravities derived from ionization equilibrium of Fe are satisfactory. There is a hint of a trend, however, in that the Cepheids with the longest periods do appear to show a deficiency of [Ti I/Fe] relative to [Ti II/Fe]. This suggests that there may be a modest degree of unaccounted-for over-ionization of Ti, presumably due to non-LTE, but the effect is minor and appears to affect only the local Cepheids.

In Figure 11, we plot the same parameters against the difference between spectroscopic and predicted gravities, ($\Delta \log g$). The three most significant outliers, with $\Delta \log\ g \leq\ -1$, are IO Cas (−1.5 dex), OT Per (−1.3 dex), and YZ Aur (−1.0 dex). Were IO Cas pulsating in the first overtone mode, the predicted fundamental period would be longer, 8.06 days, but this would reduce the discrepancy only to −1.3 dex. As noted above, the other two stars have relatively long periods, and the extreme difference between the predicted and derived gravities may be due to over-ionization, but, again, not all long period Cepheids show the same behavior.

The trends in the four panels of Figure 11 reflect those noted already in Figure 10. The [Fe/H], [Ca/Fe], and Δ[Ti/Fe] values of the outliers match those of the stars with smaller differences (when allowances are made for comparing only outer disk Cepheids amongst themselves, for reasons discussed above). The one interesting difference is that the more metal-rich local Cepheids and the more metal-poor outer disk Cepheids show differences in the sign of $\Delta \log g$. We can only speculate that this may be an artifact of systematic differences in the model atmospheres due to metallicity for such low-gravity stars.

The model atmospheres we have computed rely on the classical plane-parallel one-dimensional assumption, which may not be an adequate representation of the real atmosphere. By observing main sequence stars in the open cluster M25 (which also contains the Cepheid U Sgr), Fry & Carney (1997) investigated the reliability of classical model atmo-

spheres and whether departures from LTE affect an analysis in which LTE models are used in combination with spectroscopically derived stellar parameters. Their [Fe/H] values for the two M25 dwarfs agreed with their measured value for U Sgr. The derived metallicities also matched previous determinations of dwarfs in this cluster. They also followed several Cepheids throughout the entire pulsation cycle and found essentially identical iron abundances even as $T_{\rm eff}$ varied by over 1000 K. Identical abundance ratios for [Si/Fe], [Ca/Fe], and [Ti/Fe] were also obtained in Cepheids at different phases. Fry & Carney (1997) took this as evidence that a traditional spectroscopic analysis using classical model atmospheres can provide self-consistent and therefore reliable results for Cepheids. It is worth reiterating that Andrievsky and collaborators adopted the Fry & Carney (1997) spectroscopic $T_{\rm eff}$ scale in their analyses.

Andrievsky's concerns about a traditional spectroscopic analysis are reasonable. However, we offer four pieces of evidence suggesting that our analyses are self-consistent. First, visual inspection of the spectra suggest that HQ Per and CR Ori must have virtually identical stellar parameters (see Figure 1) which is confirmed by our analysis. Similarly, a glance at the spectra of GP Per and GV Aur suggest that their stellar parameters and/or compositions must differ (see Figure 2). Once more our analysis confirms that indeed the metallicities are different. Second, the comparison of abundances between this study and Fry & Carney (1997) as well as Andrievsky et al. reveal that the differences are small and comparable to our estimates of the measurement uncertainties. Furthermore, the abundance differences Δ[X/Fe] are not correlated with $T_{\rm eff}$ though Δ[Fe/H] may be correlated with $T_{\rm eff}$. Third, we confirm the Fry & Carney (1997) result that abundance ratios [Fe/H] and [X/Fe] are not a function of phase and/or $T_{\rm eff}$. In some cases, $T_{\rm eff}$ differs by over 1000 K. Lastly, we find that our spectroscopic gravities also produce ionization equilibrium for Ti, a species which is more susceptible to non-LTE effects than Fe due to its lower ionization potential.

4. COMPARISONS WITH OTHER STUDIES OF YOUNG STARS

4.1. Mean abundance ratios and trends with Galactocentric distance

For the iron abundances in our program Cepheids, we find a mean value [Fe/H] = -0.60 ± 0.05 ($\sigma = 0.21$). For the other abundances, we find mean values of [Mg/Fe] = 0.26 ± 0.03 ($\sigma = 0.13$), [Si/Fe] = 0.32 ± 0.02 ($\sigma = 0.10$), [Ca/Fe] = 0.18 ± 0.02 ($\sigma = 0.10$), [Ti/Fe] = 0.13 ± 0.03 ($\sigma = 0.14$), [α/Fe] = 0.20 ± 0.02 ($\sigma = 0.08$), [La/Fe] = 0.37 ± 0.03 ($\sigma = 0.13$), and [Eu/Fe] = 0.37 ± 0.03 ($\sigma = 0.12$). The program Cepheids have a mean distance 14.3 kpc ($\sigma = 1.5$ kpc). In the outer Galactic disk, our program Cepheids have subsolar ratios of [Fe/H] along with elevated ratios of [α/Fe], [La/Fe], and [Eu/Fe]. For all abundance

ratios [Fe/H] and [X/Fe], we find a large dispersion at a given Galactocentric distance. For [Fe/H], [α/Fe], [La/Fe], and [Eu/Fe], the dispersion exceeds the measurement uncertainties suggesting that the outer Galactic disk is not a well-mixed single population.

In Figures 12 and 13, we plot the abundance ratios [Fe/H] and [X/Fe] versus Galactocentric distance. By imposing a linear least squares fit to our outer disk program Cepheids which lie between 12 and 17.2 kpc, we find the following slopes and associated uncertainties: d[Fe/H]/d$R_{\rm GC}$ = -0.052 ± 0.022 dex kpc^{-1}, d[Mg/Fe]/d$R_{\rm GC}$ = 0.023 ± 0.010 dex kpc^{-1}, d[Si/Fe]/d$R_{\rm GC}$ = 0.033 ± 0.010 dex kpc^{-1}, d[Ca/Fe]/d$R_{\rm GC}$ = 0.012 ± 0.008 dex kpc^{-1}, d[Ti/Fe]/d$R_{\rm GC}$ = 0.019 ± 0.011 dex kpc^{-1}, d[α/Fe]/d$R_{\rm GC}$ = 0.016 ± 0.014 dex kpc^{-1}, d[La/Fe]/d$R_{\rm GC}$ = -0.013 ± 0.014 dex kpc^{-1}, and d[Eu/Fe]/d$R_{\rm GC}$ = 0.009 ± 0.013 dex kpc^{-1}. Some of these abundance gradients are statistically significant at the 2 or 3 σ level. However, an inspection of Figures 12 and 13 suggest that it is not clear that a linear trend is the appropriate function to apply, a caution we raised as well in Papers I and II.

4.2. Comparison with Andrievsky's Cepheid samples

Andrievsky provided a thorough account of the Cepheid abundance trends as a function of Galactocentric distance out to 15 kpc. Briefly, he and his collaborators (Andrievsky et al. 2002a,b,c; Luck et al. 2003; Andrievsky et al. 2004) suggested that the Galaxy can be divided into three zones because a single linear radial abundance gradient is inadequate to fit to the data. Zone 1 covers $4.0 \leq R_{\rm GC} \leq 6.6$, zone 2 covers $6.6 \leq R_{\rm GC} \leq 10.6$, and zone 3 covers $10.6 \leq R_{\rm GC} \leq 14.6$. Since a linear function is not supported by their data, it is more accurate to describe the global trend with Galactocentric distance as a "radial abundance distribution" even though a particular range in $R_{\rm GC}$ may be fitted with a linear function. In zone 1, the iron abundance decreases sharply with increasing Galactocentric distance with d[Fe/H]/d$R_{\rm GC}$ = -0.128 ± 0.029 dex kpc^{-1}. In zone 2, the iron abundance decreases more gradually with d[Fe/H]/d$R_{\rm GC}$ = -0.044 ± 0.004 dex kpc^{-1}. In zone 3, the iron abundance is essentially flat with d[Fe/H]/d$R_{\rm GC}$ = -0.004 ± 0.011 dex kpc^{-1}. (Note that the formal linear slope for our data more closely matches Andrievsky's zone 2 rather than their zone 3 though our Cepheids are located in zone 3 and beyond.) The mean abundance [Fe/H] for each zone was different with the mean abundance decreasing with increasing distance. Andrievsky showed that the abundance ratios [X/H] for many other elements behave similarly to [Fe/H] in these three zones. For almost all elements in each zone, the dispersion about the mean relation was low suggesting that the interstellar medium was well mixed at the time the Cepheids formed, unlike what we appear to have found in the outer disk.

4.3. Comparison with OB stars

OB stars are hot and young with lifetimes and ages comparable to the young Cepheids. They therefore offer an independent check on both the radial abundance distribution as well as the dispersion in abundance ratios.

Daflon & Cunha (2004, and references therein) measured abundances of C, N, O, Mg, Al, Si, and S in a sample of 69 young OB stars belonging to 25 open clusters, OB associations, and H II regions. These objects spanned Galactocentric distances $4.7 \leq R_{\rm GC} \leq 13.2$ kpc. Unfortunately, Fe cannot be measured in OB stars and the Daflon & Cunha (2004) sample does not extend beyond 14 kpc, the regime in which the Cepheids display a large dispersion in iron abundances. In Figure 14, we plot [α/H] versus Galactocentric distance for our Cepheids (α = Mg+Si+Ca+Ti), Andrievsky's Cepheids (α = Mg+Si+Ca+Ti), and the Daflon & Cunha (2004) sample of OB stars (α = O+Mg+Si+S). Prior to making a direct comparison between the OB stars and the Cepheids, we caution that independent analysis techniques are employed for the analysis of these different objects. There is a offset between the Cepheids and OB stars with the OB stars showing lower [α/H] by roughly 0.3 dex at a given Galactocentric distance. It is not clear if this offset is real or whether it reflects the systematic differences between the analysis techniques. For example, the much hotter OB stars are more susceptible to non-LTE effects. If this offset is real, then it would be extremely difficult to explain given the comparable ages and lifetimes of the OB stars and Cepheids. For the range of distances spanned by the OB stars, the radial abundance gradient appears rather similar between the OB stars and Cepheids. Interestingly, the most distant OB stars also appear to exhibit a dispersion in abundances. The amplitude of the dispersion is about 0.5 dex and is seen in O, Mg, and Si as well as α. The differences observed are not due to lower S/N spectra which ranged from 70 to 300.

We take two main results from the OB stars. Firstly, the abundances tend to decrease with increasing Galactocentric radius. In the range of distances covered by both the OB stars and Cepheids, the radial abundance distributions appear similar. Secondly, there is a dispersion in abundances at large distances. While there is also a scatter at smaller distances, the scatter in distant OB stars is greater than for the local OB stars. In particular, we note that the maximum dispersion is for [Si/H] and is roughly 0.8 dex, a value comparable to the amplitude of the dispersion seen in [Fe/H] in our Cepheids. Both points illustrate that the young OB stars and the young Cepheids likely have similar mean abundances, radial abundance distributions, and a dispersion in abundance ratios at a given Galactocentric distance. While the dispersion in abundance ratios may be a natural consequence of low densities in the outer Galactic disk, there are other possible explanations.

5. DISCUSSION

5.1. Introduction

In Figure 12, we show [Fe/H] and [α/Fe] versus Galactocentric distance for our sample of outer disk Cepheids. In this Figure we also include Andrievsky's sample noting that the abundance ratios have been shifted onto our system after an abundance comparison of a common subsample. (Shifts of -0.16, 0.11, 0.12, and 0.19 were applied to Andrievsky's [Fe/H], [α/Fe], [La/Fe], and [Eu/Fe] respectively.) For [Fe/H] and [α/Fe], our data appear to continue the trends with $R_{\rm GC}$ seen by Andrievsky. However, beyond $R_{\rm GC} = 14$ kpc, a subset of the sample have unusually low [Fe/H] as well as unusually high [α/Fe]. There is a hint that in the outer disk the iron abundances may have a bimodal distribution with peaks at [Fe/H] $= -0.5$ and [Fe/H] $= -0.9$ (see Figure 15). In the same Figure, the abundance ratio [α/Fe] may also exhibit a bimodal distribution. (Both distributions are somewhat sensitive to the binning. If the bin centers are shifted by half a bin width, [Fe/H] still exhibits bimodality while [α/Fe] instead shows an asymmetric distribution.) We offer two explanations for this apparent bimodality. The first possibility is that the outer disk Cepheids represent a single population which has been subject to inhomogeneous chemical evolution. Such an idea is consistent with the fact that for [Fe/H], [α/Fe], [La/Fe], and [Eu/Fe], the dispersion exceeds the measurement uncertainties. Inhomogeneous chemical evolution may be a reasonable expectation in the low density outer Galactic disk. The second possibility is that the outer disk Cepheids represent two (or more) separate populations whose star formation histories and nucleosynthetic histories are distinct despite their young ages. This suggests one or more merger events may be underway in the outer disk. Such an idea is compatible with the hierarchical assembly of galaxies predicted from "ΛCDM" cosmological simulations that successfully reproduce the observed large scale structure of the Universe.

5.2. Do the Cepheids represent a single population?

5.2.1. Expectations

Before exploring the possibility that the Cepheids represent a single population, we offer a brief discussion of plausible expectations for the chemical abundances in the outer disk.

If the outer disk has been undergoing star formation since the Galaxy formed, and has evolved essentially in isolation, with negligible amounts of infall or mergers, we expect to find the following properties. A. The outer disk Cepheids should be more metal-poor than the inner disk Cepheids, due to the slower pace of chemical evolution in these lower density

regions. Numerous chemical evolution models (e.g., Hou et al. 2000; Alibés et al. 2001; Chiappini et al. 2001) support this basic idea. B. The Cepheids should have essentially solar values of [α/Fe]. The primary factor involved in the behavior of [α/Fe] vs. [Fe/H] is the star formation rate and the time since it began. Assuming durations of star formation in the inner and outer disk, the slower star formation rate in the outer disk would have led to the appearance of SNe Ia ejecta when the [Fe/H] was still quite low. Therefore, [α/Fe] would have reached solar values after a comparable amount of time but at a lower [Fe/H]. If star formation in the outer disk began very recently, so that the contributions of SNe Ia had not had time to contribute significantly, only then would we anticipate [α/Fe] values substantially above solar, and the ages of the oldest outer disk clusters are comparable to the ages of the oldest inner disk open clusters. C. We might expect a range in [Fe/H] for the outer disk Cepheids, and among field stars and clusters of all ages, simply because of the low densities. Recall that [Fe/H] is affected by the mean distance of star-forming regions from the sources of nucleosynthesis products, but that [α/Fe] should not be so affected. D. Despite a slower pace of star formation in the outer disk compared to the solar regions, the steady progress of chemical enrichment should lead to somewhat higher mean metallicities as a function of time. The Cepheids should be at least as metal-rich as the older field red giants and old open clusters. We explore now how these predictions are or are not satisfied.

Andrievsky's sample of Cepheids already demonstrated that the inner disk Cepheids are more metal-rich than the outer disk Cepheids. In Figure 12, our distant Cepheids are considerably more metal-poor than the inner disk Cepheids. Therefore, the first expectation is satisfied.

In considering the second expectation, that the young Cepheids should have [α/Fe] $\approx$ 0 despite their low iron abundances, we again rely initially upon Andrievsky's results. His data showed that the outer disk Cepheids may have slight enhancements in [α/Fe] relative to the inner disk Cepheids. In Figure 12, our distant Cepheids have considerably higher [α/Fe] ratios than the inner disk Cepheids. Therefore, the second expectation is not confirmed by the data.

The third expectation is that the outer disk Cepheids should have a range in [Fe/H] due to the lower densities. Andrievsky's results showed that such a dispersion was not evident. For our sample of more distant Cepheids, we do find a large range in [Fe/H] as expected. However, we now need to consider whether or not the outer disk open clusters and field giants exhibit a range in [Fe/H]. A comparison between Cepheids, field stars, and open clusters is also required to assess the fourth expectation.

5.2.2. A comparison with field giants and old open clusters

In the limited samples of outer disk open clusters and field giants presented in Papers I and II, the abundance ratio [Fe/H] appeared to reach a basement value with very little dispersion about the mean value, [Fe/H] ≈ -0.5, beyond 12 kpc. Similarly, the abundance ratio [α/Fe] appeared to reach a ceiling with little dispersion about the mean value, [α/Fe] ≈ 0.2, beyond 12 kpc.

In Figure 16 we plot [Fe/H] versus Galactocentric distance for the Cepheids, open clusters, and field stars. A schematic line illustrates the behavior of the open clusters and field stars. We impose this line upon the results from the Cepheids. Within the limits of the available data, the Cepheids show more scatter in [Fe/H] in the outer disk ($R_{\rm GC} > 10$ kpc) than do the open clusters and field giants. Therefore, the dispersion in [Fe/H] seen in the outer disk Cepheids does not appear to be a feature of the open clusters and field giants and the third expectation is not completely satisfied.

The schematic line shown in Figure 16 also shows that the Cepheids reach significantly lower metallicities than do the open clusters and field stars at a given Galactocentric distance. As just described, in a "closed box" model for the evolution of the Galaxy, at the same Galactocentric distances, the metallicities of the young Cepheids must always be greater than or equal to those of the older open clusters and field stars. Therefore, the fourth expectation is not supported by the data. The failure of the data to meet this expectation offers the strongest evidence that a "closed box" model for the evolution of our Galaxy is inappropriate and that the compositions of the outer disk open clusters, field giants, and Cepheids cannot be explained as a simple evolutionary process of an isolated ensemble of stars and gas. The second and third expectations were also not satisfied.

In Figure 16, there appears to be a 0.2-0.3 dex difference between the iron abundances in the open clusters and the Andrievsky et al. Cepheids in the range centered on 8 kpc. We can attribute 0.16 dex to the offset applied to the Andrievsky Cepheids as discussed in Section 3.4. It is not clear if the remaining difference is real, perhaps as a consequence of differing ages, or a result of the analysis techniques.

We now compare the ratio [α/Fe] versus Galactocentric distance for the Cepheids, open clusters, and field stars. In Figure 17, we again show a schematic line to highlight the behavior of the open clusters and field stars and impose this line onto the Cepheids. We note that within the available data, the Cepheids show a greater scatter in [α/Fe] in the outer disk than do the open clusters and field stars. Further, a number of Cepheids reach higher [α/Fe] than do the open clusters and field stars. Elevated ratios of [α/Fe] reveal that recent star formation has occurred with Type II supernovae contributing ejecta to the interstellar

gas from which the Cepheids formed. These overabundances of [α/Fe] also suggest that Type Ia supernovae did not contribute as significantly to the outer disk's chemical evolution as is the case for local Cepheids.

For the open clusters and field stars in the outer disk, the r-process element Eu showed enhanced ratios [Eu/Fe] = 0.3 to 0.5. Since the r-process is believed to occur in massive stars, we interpreted this as confirmation that recent star formation had taken place in the outer disk when the field stars and clusters formed several Gyrs ago, as inferred from high [α/Fe]. The younger outer disk Cepheids also show enhanced ratios of [Eu/Fe] and [α/Fe] compared to the solar value. Once again we attribute the enhancements of elements synthesized in massive stars to even more recent star formation in the outer disk.

5.3. Do the Cepheids represent separate populations?

We consider now one additional dimension of complexity which may help explain our results. A simple model for the bimodality in [Fe/H] and [α/Fe] seen in Figure 15 is that the Cepheids represent different stellar populations. In Figure 16, we see that a modest majority of our program Cepheids appear to reflect a smooth transition to the inner disk Cepheids studied by Andrievsky, and we adopt a model that describes those Cepheids as having been formed within the Galactic interstellar medium. We refer to these stars as the "Galactic Cepheids". For the most metal-poor and distant Cepheids with $R_{GC} > 13.5$ kpc and [Fe/H] ≤ -0.65, we speculate that some stars may have formed under the influence of a significant on-going merger or accretion event. We refer to these stars as the "Merger Cepheids". One signature of such a merger event would be a significant difference in the chemical abundance ratios between the "Galactic Cepheids" and the "Merger Cepheids", which, recall, are independent of the distance from the sites of nucleosynthesis. Figure 18 shows that this suggested sub-sample of our program stars (the "Merger Cepheids") are very unusual. Not only are the "Merger Cepheids" more metal-poor than the larger subsample of "Galactic Cepheids", but their [α/Fe] ratios are also markedly different. The differences in the ages of Cepheids is unlikely to be even comparable to, much less longer than, the timescale for the appearance of SNe Ia in a rich star-forming environment, so these differences should reflect a major difference in the origins of the gas out of which the two sets of Cepheids formed. It seems most likely that these Cepheids are related, somehow, to the on-going merger events discussed below.

While we have described the majority of our program stars as having been formed as part of the normal evolution of the Galactic disk, we stress that Figures 16 and 17 suggest that merger and/or accretion events have been involved in the past as well. Consider Figure

16. Note that for the "Galactic Cepheids", the upper envelope of the iron abundances appears to match the basement metallicity seen in the open clusters and field stars. However, the Cepheids reach this value at larger Galactocentric distances than do the older clusters and field stars. If the absence of the gradient arises due to a succession of accretion or merger events, as discussed by Twarog et al. (1997) and Carney et al. (2005), the larger Galactocentric distance of that basement iron abundance for the younger Cepheids may be explained most readily by a growth in the Galactic disk. At the ages of the older clusters, several billion years, the edge of the Galactic disk was at 10-11 kpc, while now it is perhaps at 14 kpc or so.

We find this signature of a succession of accretion/merger events may provide an explanation for the unusual metallicities and abundance patterns we have found among the Cepheids and the older open clusters. The data suggest that the Galactic disk has grown with time, and that signs of an on-going merger event may be seen in the chemical abundance patterns of a subsample of young stars in the outer Galactic disk.

5.4. Cepheids as possible probes of rapid chemical evolution

Lower luminosity Cepheids evolve from lower luminosity main sequence stars whose lifetimes exceed those of higher luminosity main sequence stars. Therefore, higher and lower luminosity Cepheids may probe slightly different epochs of chemical enrichment with the lower luminosity Cepheids extending back to more distant times. Since luminosity and period are famously related in Cepheids, we can compare abundance ratios [Fe/H] and [X/Fe] versus period to investigate whether or not chemical evolution has occurred within the short timescales spanned by the Cepheids.

In Figure 19, we plot [Fe/H] and [α/Fe] versus period. We use different symbols to distinguish the "Galactic Cepheids" from the "Merger Cepheids". There is a hint that the "older" Cepheids (lower luminosity and therefore shorter periods) may have lower [Fe/H] and higher [α/Fe]. While our sample sizes are small, a trend may be evident within both the "Galactic" and "Merger" Cepheids. This suggests a greater contribution from Type II supernovae at earlier times and that the rate of chemical evolution is rapid. This also suggests that chemical evolution may have taken place even within the small time-frame spanned by the Cepheids. Bono et al. (2005) provide a period-age relation for Cepheids. For the metal-poor shorter period Cepheids, the lifetimes are roughly 320 million years (assuming Z = 0.004 and log P = 0.6). For the metal-rich longer period Cepheids, the lifetimes are roughly 250 million years (assuming Z = 0.01 and log P = 1.2). So the difference in ages could be as high as 70 million years for the Cepheids. The enhanced [α/Fe] and [Eu/Fe] already

signify recent star formation and the possible trend between [α/Fe] and period appear to confirm this finding. In the same Figure, we plot [La/Fe] and [Eu/Fe] though we note that the number of lines used to derive these elements is smaller than for Fe and α and therefore these abundances are subject to greater uncertainties. La and Eu do not exhibit any trends with period.

5.5. Additional clues for chemical evolution: Neutron-capture elements

That the younger Cepheids have lower metallicities than the older open clusters and field stars suggests that the outer disk cannot be described as a simple evolution of a ensemble of stars and gas. The possibly bimodal distribution for [Fe/H] and [α/Fe] displayed by the Cepheids may reflect the fact that the Cepheids are composed of different populations. We now turn to the neutron-capture elements La and Eu to see what information they provide regarding chemical evolution of the Cepheids and the merger hypothesis.

The *s*-process element La is believed to be synthesized primarily within low-mass AGB stars (e.g., see Busso et al. 1999 for a review). The elevated ratios of [La/Fe] in the outer disk show that the interstellar gas from which the outer disk Cepheids formed had been polluted by AGB stars, a result previously seen in the open clusters and field stars. We find that the "Merger Cepheids" and the "Galactic Cepheids" have similar ratios for [La/Fe], 0.30 and 0.39 respectively.

We have already noted that the *r*-process element Eu shows enhancements in the outer disk. Eu and the α elements are believed to be synthesized within massive stars and the "Merger Cepheids" and "Galactic Cepheids" showed different values for [α/Fe]. Interestingly, we note that the [Eu/Fe] ratios between the two Cepheid populations do not differ, 0.38 for the "Merger Cepheids" and 0.37 for the "Galactic Cepheids". This lack of difference may be due to the fact that Eu abundances are derived from a single line and are therefore more uncertain than the α abundances which are derived from numerous lines.

Both La and Eu exhibit considerable dispersions (as do Fe and α). In Papers I and II, we noted that the ratio [La/Eu], *s*-process to *r*-process material, also displayed a scatter in the outer disk field stars and open clusters with no objects displaying a scaled-solar pure *r*-process or pure *s*-process ratio. The Cepheids have a ratio of [La/Eu] that is centered at the solar value and exhibits a dispersion with no Cepheid having a scaled-solar pure *r*-process or pure *s*-process distribution. Elevated ratios of La and Eu were previously seen in Papers I and II and similar conclusions were drawn regarding the recent star formation and contribution of AGB stars to the chemical evolution of the outer disk. When we consider

the "Merger Cepheids" and the "Galactic Cepheids" separately, we find that the ratios of [La/Eu] are virtually identical within the uncertainties, −0.06 and −0.01 respectively.

6. CONCLUSIONS AND FUTURE WORK

In the previous two papers in this series, we presented the chemical compositions for old open cluster giants and field giants in the outer Galactic disk. In this paper we conduct an abundance analysis of 24 young Cepheids located at large Galactocentric distances. The program Cepheids therefore allow us to study the time evolution of the Galactic radial abundance distribution as well as the current radial abundance distribution.

The short lifetimes of Cepheids ensures that their compositions reflect the recent state of the ISM. In general, the abundances measured in our program Cepheids continue the trends with Galactocentric distance seen in the large sample of Cepheids analyzed by Andrievsky. We also find enhancements for [La/Fe] and [Eu/Fe] in the outer disk. For all elements, we find a scatter that exceeds the measurement uncertainties. The enhancements in [Eu/Fe] and [α/Fe] suggest that Type II supernovae have played a greater role in the chemical evolution than have Type Ia supernovae in the outer disk, compared to the inner disk. The short lifetimes of the Cepheids demonstrate that recent star formation has taken place in the outer disk. The high ratios of [La/Fe] suggest that AGB stars have also played a role in the evolution of the outer disk. We find that the ratio [La/Eu] is centered at the solar value with no star showing a scaled-solar pure s-process or r-process value.

The sample of Cepheids in the outer disk, although numbering only 24 stars, has provided some tantalizing clues to the evolution of our Galaxy. As expected, the outer disk Cepheids are on average more metal-poor than Cepheids with smaller Galactocentric distances. However, the outer disk Cepheids show higher abundances of the α elements, despite having very similar ages to Cepheids in the inner disk. The simplest conclusion to be drawn is that recent star formation in the outer disk has provided a recent enhanced production of Type II supernovae relative to Type Ia supernovae. Either the inner disk is undergoing a slower pace of chemical evolution, or there is enhanced star formation underway in the outer disk. The question would then be what is causing this phenomenon in such a low density environment?

There are two hints in the data that point toward accretion as being the underlying cause of the enhanced [α/Fe] ratios. First, the most distant Cepheids appear to have bimodal distributions of [Fe/H] and [α/Fe]. The more metal-rich Cepheids of the outer disk appear to share a similar [α/Fe] vs. [Fe/H] trend as the inner disk Cepheids. But the outlying more

metal-poor outer disk Cepheids show even higher [α/Fe] values, suggesting a separate history. Among these stars, it is intriguing that the most recently formed such star (with the longest period) has a significantly lower [α/Fe] values than the four shorter period (older) Cepheids, hinting that the sources of nucleosynthesis may have been changed on a timescale of only a few tens of millions of years. Alternately, if accretion is responsible for the difference, it may be that the four older stars formed from gas that was richer in material from a merging galaxy while the more recently formed star emerged from gas more throughly mixed with Galactic gas.

A comparison between the young Cepheids and older field stars and open cluster in the outer disk also provides clues about the evolution of the outer Galactic disk. Disregarding the apparent bimodality of the outer disk Cepheids, one must confront the observation that the younger Cepheids are more metal-poor than the older clusters and field stars. Accepting the bimodality, and concentrating on only that Cepheids that appear to continue the trend of [α/Fe] vs. [Fe/H] seen in inner disk Cepheids, one finds a behavior similar to the older clusters and field stars. [Fe/H] appears to reach a basement value of about -0.5 while [α/Fe] reaches a ceiling of $+0.15$. However, the Cepheids reach such values only for $R_{\rm GC} > 14$ kpc, while the older clusters and stars do so at 10 to 11 kpc. This suggests that the outer *stellar* disk has grown in radius by several kpc in the past several billion years. This suggests a past history of accretion, in addition to that apparently recently underway.

Accretion events have been a common theme in other recent studies of the Galaxy's outer disk. The Sloan Digital Sky Survey has detected the "Monoceros Ring" (Newberg et al. 2002). Yanny et al. (2003) have found clear dynamical evidence for a structure at $\ell = 198$, $b = -27$ that may be part of a more extensive merger remnant. The 2MASS database and its ability to distinguish M dwarfs from M giants has led to the identification of the candidate "Canis Major galaxy", whose center lies near $\ell \approx 244$, $b \approx -8$ (Martin et al. 2004, 2005; Bellazzini et al. 2004; Martínez-Delgado et al. 2005). Radial velocities of the photometrically identified streams has confirmed the existence of unique streams (Martin et al. 2005; Peñarrubia et al. 2005; Conn et al. 2005). Are any of these related to the unusual star formation history we are suggesting for the outer disk? Certainly all the evidence points to on-going accretion episodes, but how may we distinguish individual events?

The referee has drawn our attention to the fact that the metal-poor but α-rich Cepheids are not distributed as widely as the other Cepheids in Table 1. These seven stars, CI Per, EW Aur, FO Cas, GP Per, IO Cas, NY Cas, and OT Per, all lie at low Galactic latitudes (and six between $b = -2$ and -4) and between $\ell = 119$ and 166 degrees. Could these stars' locations be a clue about a possible merger origin? If there is a relation to an already-suggested merger event, its location is more consistent with Canis Major than with the

Monoceros Ring. But even so, we are reluctant to ascribe much significance to the spatial locations of these "Merger Cepheids". They are, after all, very spread out in longitude. Further, it is not clear how uniform are the searches for distant Cepheids. More extensive work in even one hemisphere than another could create such an apparent grouping (and all these Cepheids are northern ones). A more thorough search for Cepheids and, especially, the more abundant but comparably young OB stars may be needed to resolve this question.

We argue that detailed chemical composition studies such as we have undertaken here and in Papers I and II are critical to understanding the complex history of our Galaxy. Distinct chemical evolution patterns are as important, if not more so, in probing the relationship between candidate streams and merging galaxies to one another and to the stars in the outer Galactic disk. Unfortunately, little work has been done as yet. So far, only 3 stars in Canis Major have been analyzed (Sbordone et al. 2005), and the data employed had S/N=40 per pixel at 5800Å which is less than ideal (in our opinion). But the results are intriguing. The abundance ratios found by Sbordone et al. (2005) do not appear to match those seen in our samples of outer disk stars. Specifically, the Canis Major candidates have low [α/Fe] while our outer disk stars all show enhancements in [α/Fe]. Low abundances of [α/Fe] are a signature of the current dwarf spheroidals orbiting our Galaxy (Venn et al. 2004). Enhancements in [α/Fe] in the "Merger Cepheids" may therefore suggest that these Cepheids formed as a result of star formation triggered by the merger rather than forming within the dwarf galaxy. Unfortunately, detailed stellar abundance ratios are unable to offer a clearer picture of the exact mechanism. While we speculate that the star formation was triggered by merging gas, we cannot say whether that gas was pristine or pre-enriched. Detailed abundance ratios in a large sample of candidate members of the Monoceros ring and/or Canis Major Galaxy are required. The measured abundance ratios would confirm if the outer disk has been growing via the merger of dwarf galaxies as well as providing the chemical history of these small galaxies. Such a result would have profound implications not only for our understanding of the evolution of our Galaxy but also for ΛCDM cosmology.

We thank the anonymous referee for many helpful suggestions and comments. We are extremely grateful to the National Science Foundation for their financial support through grants grants AST 96-19381, AST 99-88156, and AST 03-05431 to the University of North Carolina.

Table 1. Program stars.

Name	Source[a]	RA J2000.0	Dec J2000.0	l (deg)	b (deg)	Period d	Exposure Time (s)	S/N[b]	HJD −2,450,000	Phase	$< V >$ (mag)	$< K >$ CIT	E(B-V)	R_{GC} kpc
CE Pup	C	08 14 08.0	−42 34 05	259.2	−4.4	49.53	6000	77	1206.8201	0.434	11.96	7.533	0.74	15.4
CI Per	D	02 05 02.3	+57 08 35	132.8	−4.3	3.38	7200	85	0811.6732	0.963	12.68	10.332	0.28	14.0
CR Ori	M	06 05 44.9	+13 14 23	195.9	−3.9	4.91	3600	60	1206.5626	0.687	12.30	9.195	0.56	13.2
CU Mon	D	06 32 46.8	+00 02 35	210.8	−4.1	4.71	7200	85	1205.5528	0.809	13.63	9.894	0.79	14.4
CY Aur	D	04 57 40.1	+46 05 33	160.5	2.0	13.85	1800	42	0809.8810	0.128	11.89	7.716	0.81	13.1
EE Mon	M	06 50 48.7	−07 58 50	220.0	−3.8	4.81	7200	85	0832.7457	0.467	12.50	10.141	0.49	15.3
ER Aur	D	05 13 10.0	+41 59 26	165.5	1.7	15.69	1800	42	0809.7541	0.859	11.53	8.480	0.52	16.5
EW Aur	D	04 51 24.9	+38 11 19	166.0	−3.9	2.66	9600	98	1184.7479	0.526	13.53	10.392	0.63	13.9
FI Mon	M	07 10 38.1	−07 07 22	221.5	1.0	3.29	3600	60	0834.7697	0.930	12.93	9.632	0.54	12.2
FO Cas	D	00 17 02.6	+60 48 10	118.8	−1.8	6.80	14400	120	1183.5900	0.454	14.33	10.531	0.82	17.2
GP Per	D	04 23 19.3	+44 14 12	157.9	−3.8	2.04	7200	85	1186.5814	0.674	14.10	10.823	0.74	13.8
GV Aur	D	05 44 14.1	+37 35 12	172.5	4.3	5.26	1800	42	0809.7890	0.171	12.09	8.821	0.58	12.7
HQ Car	C	10 20 32.0	−61 14 58	285.8	−3.5	14.07	3300	57	0834.8637	0.361	12.25	9.937	0.42	15.7
HQ Per	D	04 43 58.0	+40 50 05	163.0	−3.3	8.64	5400	73	0811.7616	0.622	11.61	8.410	0.59	13.3
HW Pup	M	07 57 42.3	−27 36 07	244.8	0.8	13.45	2400	49	0831.7934	0.585	12.13	8.773	0.72	14.0
IN Aur	D	05 15 27.3	+37 22 21	169.5	−0.6	4.91	7200	85	1186.6843	0.266	13.83	9.854	0.95	14.8
IO Cas	D	01 47 02.8	+59 36 23	129.9	−2.5	5.60	10800	104	1185.5775	0.787	13.70	10.544	0.61	17.1
NT Pup	C	07 58 46.3	−38 59 40	254.6	−5.0	15.57	3600	60	0832.8380	0.792	12.14	8.134	0.67	12.0
NY Cas[c]	D	00 40 23.3	+58 37 07	121.5	−4.2	4.01	7200	85	0809.6238	0.233	13.34	10.927	0.35	16.4
OT Per	D	04 38 37.9	+47 44 24	157.2	0.6	26.09	4800	69	1185.7099	0.468	13.53	7.649	1.44	14.9
V484 Mon	D	06 31 05.4	−02 08 48	212.5	−5.5	3.14	14400	120	1203.6105	0.069	13.76	10.499	0.71	14.4
WW Mon	D	06 33 37.3	+09 12 13	202.7	0.3	4.66	3600	60	0809.8249	0.399	12.55	9.510	0.64	13.6
XZ CMa	C	07 00 24.9	−20 25 54	232.2	−7.3	2.56	3600	60	0834.8182	0.292	12.76	10.491	0.27	13.0
YZ Aur	D	05 15 22.1	+40 04 41	167.3	0.9	18.19	2400	49	1186.7698	0.219	10.36	6.717	0.57	12.1

[a]C = Caldwell & Coulson (1987), D = DDO electronic database, M = Metzger et al. (1998)

[b]S/N ratio the peak value per pixel in the order containing H_α.

[c]We corrected the observed period from 2.82d to 4.01d since this star is an overtone pulsator.

Table 2. Line list

Wavelength(Å)	Species	LEP(eV)	log gf	Wavelength(Å)	Species	LEP(eV)	log gf	Wavelength(Å)	Species	LEP(eV)	log gf
5711.09	Mg I	4.35	−1.830	5151.91	Fe I	1.01	−3.320	6355.03	Fe I	2.84	−2.400
5645.61	Si I	4.93	−2.140	5166.28	Fe I	0.00	−4.200	6393.60	Fe I	2.43	−1.470
5665.56	Si I	4.92	−2.040	5198.71	Fe I	2.22	−2.140	6408.02	Fe I	3.68	−1.070
5690.43	Si I	4.93	−1.870	5217.39	Fe I	3.21	−1.180	6411.65	Fe I	3.65	−0.730
5708.40	Si I	4.95	−1.470	5242.49	Fe I	3.63	−0.980	6430.84	Fe I	2.17	−2.010
5772.15	Si I	5.08	−1.750	5253.46	Fe I	3.28	−1.630	6494.98	Fe I	2.40	−1.270
5793.07	Si I	4.93	−2.060	5288.53	Fe I	3.69	−1.530	6518.36	Fe I	2.83	−2.500
5948.54	Si I	5.08	−1.230	5302.30	Fe I	3.28	−0.770	6574.23	Fe I	0.99	−5.000
6125.02	Si I	5.61	−1.480	5307.36	Fe I	1.61	−2.990	6575.02	Fe I	2.59	−2.730
6145.01	Si I	5.62	−1.380	5321.11	Fe I	4.43	−1.110	6581.21	Fe I	1.48	−4.710
6155.13	Si I	5.62	−0.700	5339.93	Fe I	3.26	−0.740	6592.91	Fe I	2.73	−1.490
5349.47	Ca I	2.71	−0.310	5367.48	Fe I	4.41	0.430	6593.87	Fe I	2.43	−2.420
5512.98	Ca I	2.93	−0.460	5379.57	Fe I	3.69	−1.530	6609.11	Fe I	2.56	−2.690
5581.97	Ca I	2.52	−0.560	5415.19	Fe I	4.38	0.630	6625.02	Fe I	1.01	−5.370
5588.76	Ca I	2.53	0.360	5497.52	Fe I	1.01	−2.850	6677.99	Fe I	2.69	−1.440
5590.12	Ca I	2.52	−0.570	5506.78	Fe I	0.99	−2.800	6750.15	Fe I	2.42	−2.620
5594.47	Ca I	2.52	0.100	5569.62	Fe I	3.41	−0.540	6752.70	Fe I	4.64	−1.270
5598.49	Ca I	2.52	−0.090	5586.76	Fe I	3.37	−0.160	6810.26	Fe I	4.60	−1.000
5601.28	Ca I	2.53	−0.520	5600.23	Fe I	4.26	−1.490	6945.20	Fe I	2.42	−2.480
6166.44	Ca I	2.52	−1.140	5618.63	Fe I	4.21	−1.290	7112.17	Fe I	2.99	−3.040
6449.81	Ca I	2.52	−0.500	5624.54	Fe I	3.41	−0.800	7401.69	Fe I	4.18	−1.660
6471.66	Ca I	2.53	−0.690	5701.55	Fe I	2.56	−2.220	7511.01	Fe I	4.18	0.080
6493.78	Ca I	2.52	−0.110	5753.12	Fe I	4.26	−0.710	7710.36	Fe I	4.22	−1.130
6499.65	Ca I	2.52	−0.820	5775.08	Fe I	4.22	−1.310	7941.09	Fe I	3.27	−2.330
6717.69	Ca I	2.71	−0.520	5816.37	Fe I	4.55	−0.620	4993.36	Fe II	2.81	−3.490
7148.15	Ca I	2.71	0.140	5855.09	Fe I	4.60	−1.550	5100.66	Fe II	2.81	−4.140
7202.19	Ca I	2.71	−0.260	5956.69	Fe I	0.86	−4.610	5132.67	Fe II	2.81	−3.900
4999.50	Ti I	0.83	0.310	6012.21	Fe I	2.22	−4.070	5325.55	Fe II	3.22	−3.220
5007.21	Ti I	0.82	0.170	6027.05	Fe I	4.07	−1.110	5414.07	Fe II	3.22	−3.750
5016.16	Ti I	0.85	−0.520	6065.48	Fe I	2.61	−1.530	5425.26	Fe II	3.20	−3.370
5024.84	Ti I	0.82	−0.550	6082.71	Fe I	2.22	−3.570	5732.72	Fe II	3.38	−4.670
5173.74	Ti I	0.00	−1.060	6136.62	Fe I	2.45	−1.400	5991.38	Fe II	3.15	−3.560
5210.39	Ti I	0.05	−0.830	6151.62	Fe I	2.17	−3.300	6084.11	Fe II	3.20	−3.810
6126.22	Ti I	1.05	−1.370	6165.36	Fe I	4.14	−1.490	6149.26	Fe II	3.89	−2.720
6258.10	Ti I	1.44	−0.300	6173.34	Fe I	2.22	−2.880	6179.38	Fe II	5.57	−2.600
6261.11	Ti I	1.43	−0.420	6180.20	Fe I	2.73	−2.640	6247.56	Fe II	3.89	−2.330
6554.22	Ti I	1.46	−1.020	6200.31	Fe I	2.61	−2.440	6369.46	Fe II	2.89	−4.250
5268.62	Ti II	2.60	−1.620	6219.28	Fe I	2.20	−2.430	6383.72	Fe II	5.55	−2.270
5381.02	Ti II	1.57	−2.080	6229.23	Fe I	2.84	−2.850	6416.92	Fe II	3.89	−2.740
5418.80	Ti II	1.58	−1.860	6230.73	Fe I	2.56	−1.280	6432.68	Fe II	2.89	−3.710
5910.05	Ti II	1.57	−3.240	6232.64	Fe I	3.65	−1.280	6516.08	Fe II	2.89	−3.450
6606.95	Ti II	2.06	−2.790	6246.32	Fe I	3.60	−0.890	7222.39	Fe II	3.89	−3.300
7214.72	Ti II	2.59	−1.750	6252.55	Fe I	2.40	−1.690	7479.69	Fe II	3.89	−3.590
4924.77	Fe I	2.28	−2.290	6265.13	Fe I	2.17	−2.550	7515.83	Fe II	3.90	−3.430
4930.31	Fe I	3.96	−1.260	6297.79	Fe I	2.22	−2.740	7711.72	Fe II	3.90	−2.540
5014.94	Fe I	3.94	−0.320	6301.50	Fe I	3.65	−0.770	5769.06	La II	1.25	−0.690
5044.21	Fe I	2.85	−2.030	6322.69	Fe I	2.59	−2.430	5805.77	La II	0.13	−1.560
5049.82	Fe I	2.28	−1.370	6335.33	Fe I	2.20	−2.190	6262.29	La II	0.40	−1.220
5083.34	Fe I	0.96	−2.960	6336.82	Fe I	3.68	−0.920	6390.48	La II	0.32	−1.410
5141.74	Fe I	2.42	−2.000	6344.15	Fe I	2.43	−2.920	6645.13	Eu II	1.38	0.200

Table 3. Atmospheric parameters.

Name	$T_{\rm eff}$(K)	$\log g$	ξ_t	$\log \epsilon$(Fe I)	σ	N	$\log \epsilon$(Fe II)	σ	N	[Fe/H]
CE Pup	4975	0.20	4.05	7.13	0.15	26	7.15	0.04	4	−0.40
CI Per	6000	1.50	3.35	6.50	0.26	23	6.50	0.24	8	−1.04
CR Ori	5625	1.30	3.17	6.94	0.09	24	6.98	0.11	10	−0.58
CU Mon	5975	1.30	2.95	6.97	0.12	30	6.99	0.09	9	−0.56
CY Aur	5225	0.80	2.72	7.02	0.11	35	7.05	0.10	8	−0.51
EE Mon	5900	1.50	2.77	7.00	0.10	33	7.02	0.17	9	−0.53
ER Aur	5725	1.00	2.90	6.91	0.11	49	6.90	0.17	16	−0.64
EW Aur	6200	1.30	2.88	6.61	0.12	31	6.68	0.18	11	−0.90
FI Mon	6700	1.90	3.35	7.21	0.13	21	7.18	0.17	9	−0.35
FO Cas	6300	1.00	2.84	6.64	0.14	40	6.65	0.17	17	−0.90
GP Per	6400	1.50	2.69	6.65	0.15	38	6.66	0.15	15	−0.89
GV Aur	6400	1.70	2.83	7.29	0.14	48	7.26	0.16	16	−0.27
HQ Car	5400	0.80	3.15	7.11	0.13	32	7.16	0.12	9	−0.41
HQ Per	5625	1.70	4.85	7.07	0.15	32	7.08	0.13	8	−0.47
HW Pup	5750	1.00	3.09	7.12	0.11	26	7.16	0.14	10	−0.40
IN Aur	6100	1.80	3.39	7.02	0.13	46	7.03	0.15	11	−0.52
IO Cas	5225	0.30	3.11	6.75	0.09	26	6.73	0.12	8	−0.80
NT Pup	5250	0.80	3.42	7.18	0.17	35	7.21	0.11	9	−0.35
NY Cas	6050	1.70	2.62	6.85	0.14	45	6.83	0.18	18	−0.70
OT Per	4700	−0.30	5.40	6.64	0.18	29	6.69	0.11	8	−0.88
V484 Mon	6550	1.70	2.98	7.08	0.11	23	7.08	0.15	11	−0.46
WW Mon	6300	1.50	2.86	6.96	0.12	36	6.94	0.13	14	−0.59
XZ CMa	6750	1.70	3.32	6.97	0.15	20	6.97	0.13	9	−0.57
YZ Aur	5325	0.20	2.88	6.89	0.16	32	6.92	0.20	11	−0.64

Table 4. Mean stellar abundances.

Name	[Mg/Fe][a]	[Si/Fe]	σ	N	[Ca/Fe]	σ	N	[Ti I/Fe]	σ	N	[Ti II/Fe]	σ	N	[α/Fe]	[La/Fe]	σ	N	[Eu/Fe][a]
CE Pup	...	0.30	0.17	10	0.19	0.06	2	0.16	0.16	6	0.12	0.00	2	0.19	0.43	0.06	4	0.45
CI Per	...	...	...	...	0.34	0.16	9	...	...	...	0.25	0.04	2	0.30	...	...	...	...
CR Ori	0.29	0.28	0.11	7	0.22	0.17	9	0.25	0.00	1	0.10	0.07	3	0.23	0.51	0.05	4	0.43
CU Mon	...	0.32	0.13	5	0.19	0.15	9	0.26	...	1	0.19	...	1	0.24	0.39	0.05	3	0.41
CY Aur	0.38	0.27	0.12	9	0.11	0.05	5	0.07	0.19	8	0.21	0.07	4	0.21	0.50	0.20	4	0.41
EE Mon	0.17	0.33	0.20	8	0.12	0.17	8	0.10	0.11	2	−0.07	0.18	2	0.13	0.32	0.04	4	0.48
ER Aur	0.23	0.36	0.18	9	0.15	0.13	12	0.17	0.26	9	0.00	0.11	5	0.18	0.39	0.05	4	0.49
EW Aur	0.31	0.56	...	1	0.27	0.20	8	0.33	0.25	4	0.28	0.21	4	0.35	...	...	...	0.20
FI Mon	0.21	0.25	0.13	3	0.28	0.21	3	...	...	...	...	...	...	0.25	0.29	...	1	...
FO Cas	0.27	0.46	0.08	4	0.22	0.16	15	0.39	0.33	4	0.26	0.30	6	0.32	...	...	...	0.40
GP Per	...	0.26	0.06	2	0.24	0.20	9	...	...	...	0.46	0.14	4	0.32	...	...	...	...
GV Aur	0.01	0.17	0.16	8	0.15	0.15	15	0.14	0.17	7	0.09	0.22	6	0.11	0.51	0.05	3	0.37
HQ Car	...	0.44	0.18	9	−0.04	0.22	6	−0.01	...	1	−0.07	...	1	0.08	...	...	...	0.06
HQ Per	0.18	0.14	0.22	6	0.04	0.12	7	0.12	0.09	3	0.16	0.15	3	0.13	0.44	...	1	0.52
HW Pup	0.16	0.44	0.12	4	0.09	0.07	6	0.06	0.11	2	−0.05	0.01	2	0.14	0.39	0.03	3	0.27
IN Aur	0.27	0.24	0.19	5	0.12	0.13	9	−0.02	0.05	5	−0.08	0.00	2	0.11	0.49	...	1	0.42
IO Cas	0.45	0.50	0.15	5	0.40	0.21	6	0.23	0.13	4	−0.01	0.14	4	0.31	0.03	0.09	2	0.25
NT Pup	0.09	0.23	0.11	9	0.03	0.07	6	0.01	0.24	5	0.09	0.07	2	0.09	0.38	0.09	2	0.33
NY Cas	0.47	0.25	0.10	4	0.26	0.18	14	0.36	0.24	5	0.29	0.22	6	0.33	0.58	...	1	0.55
OT Per	...	0.37	0.14	8	0.05	0.21	5	−0.01	0.31	7	0.11	0.11	3	0.13	0.30	0.15	3	0.43
V484 Mon	0.09	0.33	0.13	7	0.21	0.14	8	0.19	0.10	2	0.05	0.05	2	0.17	0.33	...	1	0.51
WW Mon	0.33	0.33	0.26	6	0.23	0.15	14	0.10	0.05	3	−0.06	0.05	4	0.19	0.23	0.11	3	0.32
XZ CMa	...	0.37	0.16	3	0.14	0.14	4	...	...	...	0.11	...	1	0.21	...	...	...	...
YZ Aur	0.47	0.30	0.11	9	0.17	0.08	6	−0.02	0.07	4	−0.24	0.11	4	0.13	0.24	0.08	4	0.24

[a]Mg and Eu abundances were derived from 1 line.

Table 5. Abundance dependences on model parameters for ER Aur.

Species	$T_{\rm eff}$ + 100	$\log g$ + 0.3	ξ_t + 0.3
[Mg/Fe]	−0.01	−0.06	0.03
[Si/Fe]	0.01	−0.05	0.05
[Ca/Fe]	0.03	−0.05	0.02
[Ti I/Fe]	0.07	−0.06	0.01
[Ti II/Fe]	−0.03	0.06	−0.01
[α/Fe]	0.01	−0.03	0.02
[Fe I/H]	0.13	−0.02	−0.05
[Fe II/H]	0.02	0.10	−0.06
[La/Fe]	0.01	0.06	0.05
[Eu/Fe]	−0.01	0.06	0.04

Table 6. Stellar parameters and abundances for nearby Cepheids also studied by Fry & Carney and Andrievsky.

Name	Phase	$T_{\rm eff}$	$\log g$	ξ_t	[Fe/H]	[Mg/Fe]	[Si/Fe]	[Ca/Fe]	[Ti I/Fe]	[Ti II/Fe]	[α/Fe]	[La/Fe]	[Eu/Fe]
RX Aur	0.304	5400	1.1	3.30	−0.27	0.06	0.24	0.01	0.11	0.18	0.12	0.47	0.42
RX Aur	0.217	5550	1.3	3.10	−0.28	0.05	0.18	0.05	...	0.11	0.10	0.50	0.38
Del Cep	0.399	5700	1.7	2.85	−0.08	−0.13	0.13	0.00	0.04	0.09	0.03	0.46	0.28
Del Cep	0.950	6850	2.2	2.75	0.05	−0.05	0.12	0.06	0.12	0.04	0.06	0.36	0.25
X Cyg	0.432	4875	0.7	3.31	−0.16	0.19	0.13	0.00	−0.02	...	0.07	0.34	0.25
X Cyg	0.615	4950	1.1	4.75	−0.09	...	0.02	−0.15	0.07	0.09	0.01	0.39	0.19
Zet Gem	0.410	5300	1.5	3.55	−0.07	0.12	0.15	−0.05	0.05	0.15	0.08	0.33	0.27
Zet Gem	0.806	5700	1.4	3.05	−0.07	0.11	0.18	0.06	−0.04	0.02	0.07	0.39	0.24
S Sge	0.463	5550	1.4	3.16	−0.11	0.08	0.18	0.01	−0.02	0.07	0.06	0.25	0.21
S Sge	0.940	6400	1.8	2.77	−0.08	−0.03	0.11	0.02	0.01	−0.11	0.00	0.34	0.23
SZ Tau	0.333	6000	1.7	2.51	−0.04	−0.03	0.16	0.05	0.06	−0.04	0.04	0.32	0.19
SZ Tau	0.603	5725	1.5	2.45	−0.15	0.02	0.12	0.06	0.01	−0.05	0.03	0.28	0.15
SV Vul	0.283	5150	0.2	3.39	−0.13	0.23	0.23	0.01	0.00	0.16	0.12	0.25	0.28
SV Vul	0.371	5050	0.2	3.28	−0.11	...	0.25	0.00	−0.01	0.23	0.12	0.24	0.27
Eta Aql	0.955	6575	2.3	3.24	0.07	−0.05	0.05	0.00	0.17	0.05	0.04	0.41	0.28
T Mon	0.387	4950	0.4	3.65	−0.15	0.02	0.10	0.03	−0.03	0.27	0.08	0.25	0.25
T Vul	0.011	6575	2.0	3.03	−0.15	0.00	0.15	0.03	0.00	0.04	0.04	0.38	0.30
U Sgr	0.958	6450	2.1	3.40	−0.08	−0.04	0.00	0.08	0.06	0.07	0.03	0.33	0.18
U Sgr	0.404	5550	1.5	3.21	−0.09	0.04	0.13	−0.03	−0.01	0.01	0.03	0.25	0.19

REFERENCES

Alcock, C., Allsman, R. A., Axelrod, T. S., Bennett, D. P., Cook, K. H., Freeman, K. C., Griest, K., Marshall, S. L., Peterson, B. A., Pratt, M. R., Quinn, P. J., Reimann, J., Rodgers, A. W., Stubbs, C. W., Sutherland, W., & Welch, D. L. 1995, AJ, 109, 1653

Alibés, A., Labay, J., & Canal, R. 2001, A&A submitted (astro-ph/0107016)

Andrievsky, S. M., Bersier, D., Kovtyukh, V. V., Luck, R. E., Maciel, W. J., Lépine, J. R. D., & Beletsky, Y. V. 2002a, A&A, 384, 140

Andrievsky, S. M., Kovtyukh, V. V., Luck, R. E., Lépine, J. R. D., Bersier, D., Maciel, W. J., Barbuy, B., Klochkova, V. G., Panchuk, V. E., & Karpischek, R. U. 2002b, A&A, 381, 32

Andrievsky, S. M., Kovtyukh, V. V., Luck, R. E., Lépine, J. R. D., Maciel, W. J., & Beletsky, Y. V. 2002c, A&A, 392, 491

Andrievsky, S. M., Luck, R. E., Martin, P., & Lépine, J. R. D. 2004, A&A, 413, 159

Bellazzini, M., Ibata, R., Monaco, L., Martin, N., Irwin, M. J., & Lewis, G. F. 2004, MNRAS, 354, 1263

Biémont, E., Baudoux, M., Kurucz, R. L., Ansbacher, W., & Pinnington, E. H. 1991, A&A, 249, 539

Blackwell, D. E., Booth, A. J., Haddock, D. J., Petford, A. D., & Leggett, S. K. 1986a, MNRAS, 220, 549

Blackwell, D. E., Booth, A. J., Menon, S. L. R., & Petford, A. D. 1986b, MNRAS, 220, 289

Blackwell, D. E., Ibbetson, P. A., Petford, A. D., & Shallis, M. J. 1979a, MNRAS, 186, 633

Blackwell, D. E., Lynas-Gray, A. E., & Smith, G. 1995, A&A, 296, 217

Blackwell, D. E., Menon, S. L. R., & Petford, A. D. 1983, MNRAS, 204, 883

Blackwell, D. E., Menon, S. L. R., Petford, A. D., & Shallis, M. J. 1982, MNRAS, 201, 611

Blackwell, D. E., Petford, A. D., & Shallis, M. J. 1979b, MNRAS, 186, 657

Blackwell, D. E., Petford, A. D., Shallis, M. J., & Simmons, G. J. 1980, MNRAS, 191, 445

Bono, G., Marconi, M., Cassisi, S., Caputo, F., Gieren, W., & Pietrzynski, G. 2005, ApJ, 621, 966

Busso, M., Gallino, R., & Wasserburg, G. J. 1999, ARA&A, 37, 239

Caldwell, J. A. R. & Coulson, I. M. 1987, AJ, 93, 1090

Carney, B. W., Yong, D., de Almeida, L., & Seitzer, P. 2005, AJ in press (astro-ph/0506210)

Carpenter, J. M. 2001, AJ, 121, 2851

Chiappini, C., Matteucci, F., & Romano, D. 2001, ApJ, 554, 1044

Conn, B. C., Martin, N. F., Lewis, G. F., Ibata, R. A., Bellazzini, M., & Irwin, M. J. 2005, MNRAS, L87

Daflon, S. & Cunha, K. 2004, ApJ, 617, 1115

Edvardsson, B., Andersen, J., Gustafsson, B., Lambert, D. L., Nissen, P. E., & Tomkin, J. 1993, A&A, 275, 101

Fernie, J. D. 1990, ApJS, 72, 153

—. 1995, AJ, 110, 2361

Friel, E. D. 1995, ARA&A, 33, 381

—. 2005, Chemical Abundances and Mixing in Stars in the Milky Way and its Satellites (ed. L. Pasquini and S. Randich (Springer-Verlag), in press)

Fry, A. M. & Carney, B. W. 1997, AJ, 113, 1073

Henry, R. B. C., Kwitter, K. B., & Balick, B. 2004, AJ, 127, 2284

Hou, J. L., Prantzos, N., & Boissier, S. 2000, A&A, 362, 921

Ibata, R. A., Irwin, M. J., Lewis, G. F., Ferguson, A. M. N., & Tanvir, N. 2003, MNRAS, 340, L21

Kovtyukh, V. V. & Andrievsky, S. M. 1999, A&A, 351, 597

Kovtyukh, V. V. & Gorlova, N. I. 2000, A&A, 358, 587

Kurucz, R. 1993, ATLAS9 Stellar Atmosphere Programs and 2 km/s grid. Kurucz CD-ROM No. 13. Cambridge, Mass.: Smithsonian Astrophysical Observatory, 1993., 13

Lawler, J. E., Bonvallet, G., & Sneden, C. 2001a, ApJ, 556, 452

Lawler, J. E., Wickliffe, M. E., den Hartog, E. A., & Sneden, C. 2001b, ApJ, 563, 1075

Luck, R. E., Gieren, W. P., Andrievsky, S. M., Kovtyukh, V. V., Fouqué, P., Pont, F., & Kienzle, F. 2003, A&A, 401, 939

Luck, R. E. & Lambert, D. L. 1985, ApJ, 298, 782

Madore, B. F. & Freedman, W. L. 1991, PASP, 103, 933

Martin, N. F., Ibata, R. A., Bellazzini, M., Irwin, M. J., Lewis, G. F., & Dehnen, W. 2004, MNRAS, 348, 12

Martin, N. F., Ibata, R. A., Conn, B. C., Lewis, G. F., Bellazzini, M., & Irwin, M. J. 2005, MNRAS, 362, 906

Martínez-Delgado, D., Penarrubia, J., Dinescu, D. I., Butler, D. J., & Rix, H. W. 2005, astro-ph/0506012

Metzger, M. R., Caldwell, J. A. R., & Schechter, P. L. 1998, AJ, 115, 635

Newberg, H. J., Yanny, B., Rockosi, C., Grebel, E. K., Rix, H., Brinkmann, J., Csabai, I., Hennessy, G., Hindsley, R. B., Ibata, R., Ivezić, Z., Lamb, D., Nash, E. T., Odenkirchen, M., Rave, H. A., Schneider, D. P., Smith, J. A., Stolte, A., & York, D. G. 2002, ApJ, 569, 245

Peñarrubia, J., Martínez-Delgado, D., Rix, H. W., Gómez-Flechoso, M. A., Munn, J., Newberg, H., Bell, E. F., Yanny, B., Zucker, D., & Grebel, E. K. 2005, ApJ, 626, 128

Ramírez, S. V. & Cohen, J. G. 2002, AJ, 123, 3277

Reddy, B. E., Tomkin, J., Lambert, D. L., & Allende Prieto, C. 2003, MNRAS, 340, 304

Sbordone, L., Bonifacio, P., Marconi, G., Zaggia, S., & Buonanno, R. 2005, A&A, 430, L13

Schlegel, D. J., Finkbeiner, D. P., & Davis, M. 1998, ApJ, 500, 525

Shaver, P. A., McGee, R. X., Newton, L. M., Danks, A. C., & Pottasch, S. R. 1983, MNRAS, 204, 53

Smith, G. & Raggett, D. S. J. 1981, Journal of Physics B Atomic Molecular Physics, 14, 4015

Sneden, C. 1973, ApJ, 184, 839

Soszynski, I., Gieren, W., & Pietrzynski, G. 2005, PASP submitted (astro-ph/0503598)

Twarog, B. A., Ashman, K. M., & Anthony-Twarog, B. J. 1997, AJ, 114, 2556

Venn, K. A., Irwin, M., Shetrone, M. D., Tout, C. A., Hill, V., & Tolstoy, E. 2004, AJ, 128, 1177

Yanny, B., Newberg, H. J., Grebel, E. K., Kent, S., Odenkirchen, M., Rockosi, C. M., Schlegel, D., Subbarao, M., Brinkmann, J., Fukugita, M., Ivezic, Ž., Lamb, D. Q., Schneider, D. P., & York, D. G. 2003, ApJ, 588, 824

Yong, D., Carney, B. W., & de Almeida, L. 2005, AJ in press (astro-ph/0504193)

This preprint was prepared with the AAS LaTeX macros v5.2.

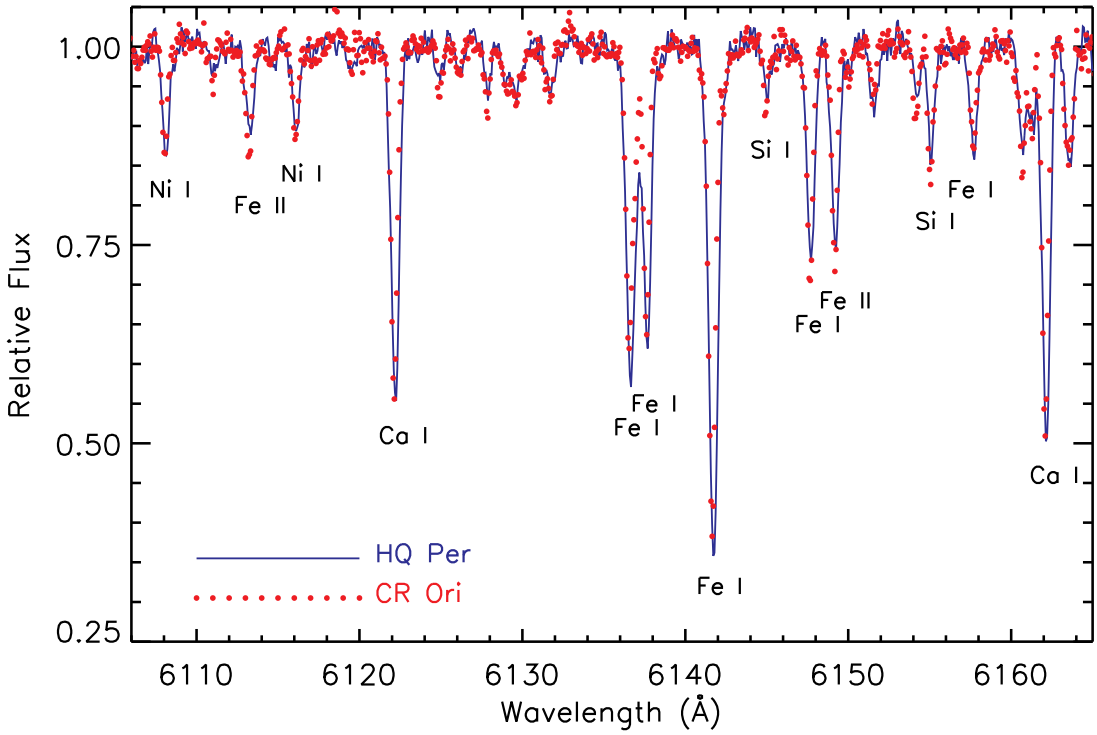

Fig. 1.— Spectra of HQ Per ($R_{\rm GC}$ = 13.3 kpc) and CR Ori ($R_{\rm GC}$ = 13.2 kpc) between 6110 and 6160Å. The spectra are very similar suggesting that these Cepheids likely have comparable stellar parameters and abundances.

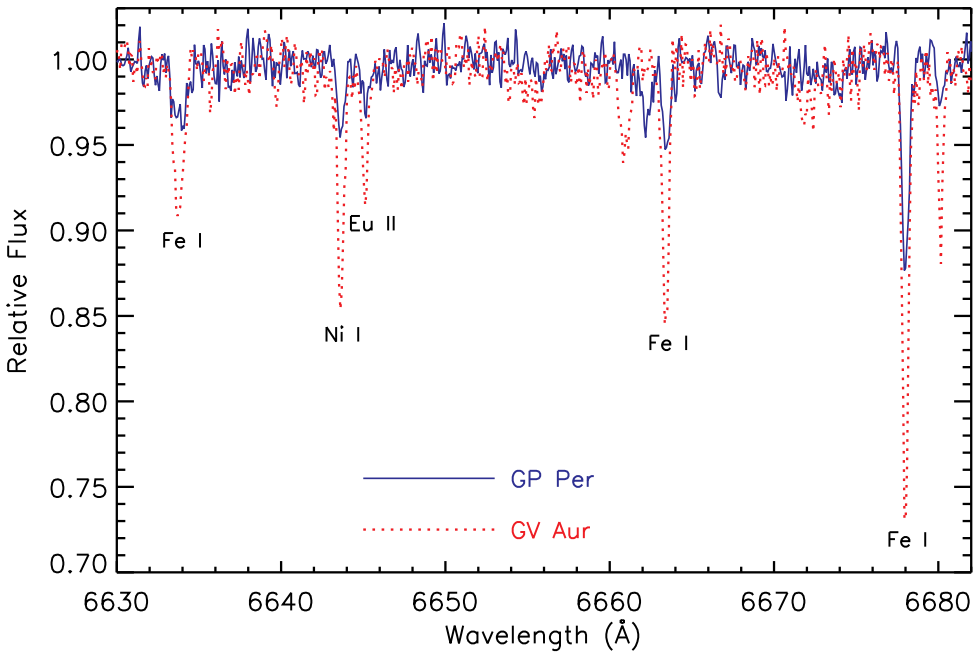

Fig. 2.— Spectra of GP Per and GV Aur near the 6645Å Eu line. The Cepheids have identical effective temperatures $T_{\rm eff}$ = 6400K so the contrasting line strengths reflect real abundance differences.

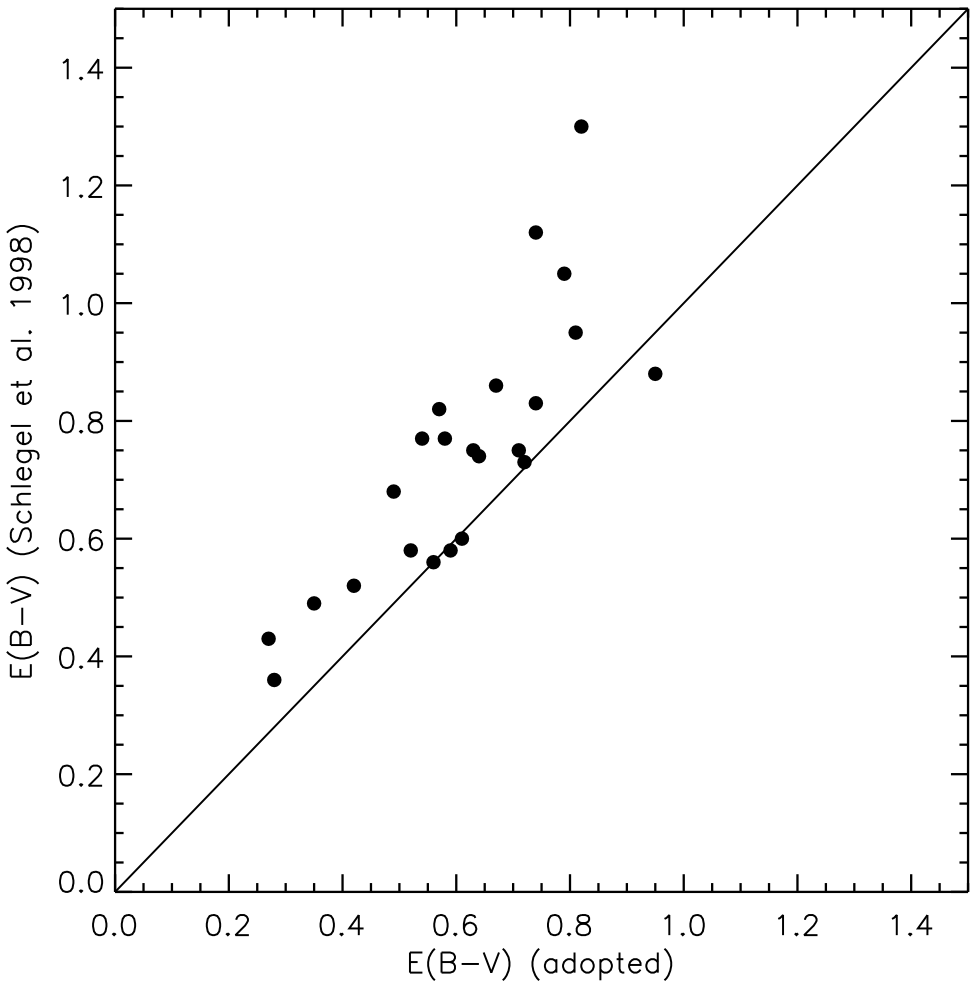

Fig. 3.— Comparison of the reddening E(B-V) between our adopted values and those from Schlegel et al. (1998).

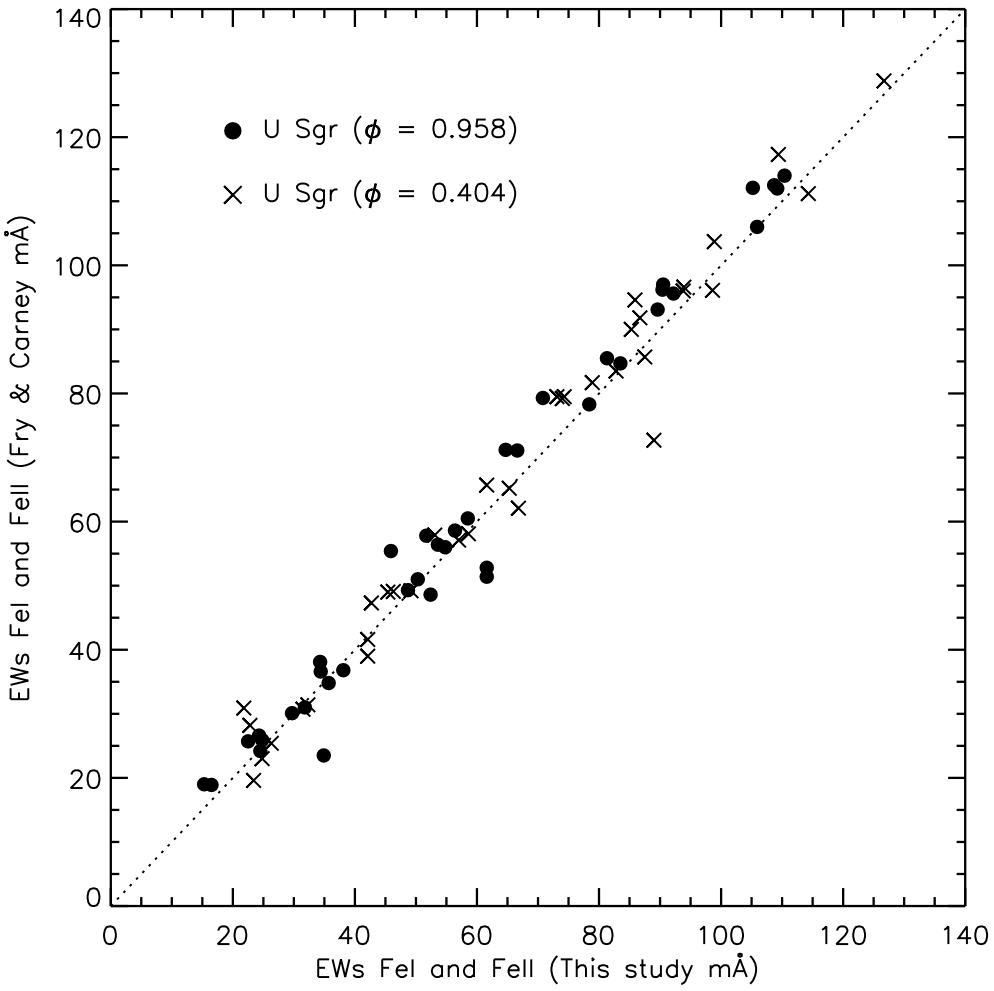

Fig. 4.— Comparison of the EWs of Fe I and Fe II lines between this study and Fry & Carney (1997) for U Sgr at two different phases.

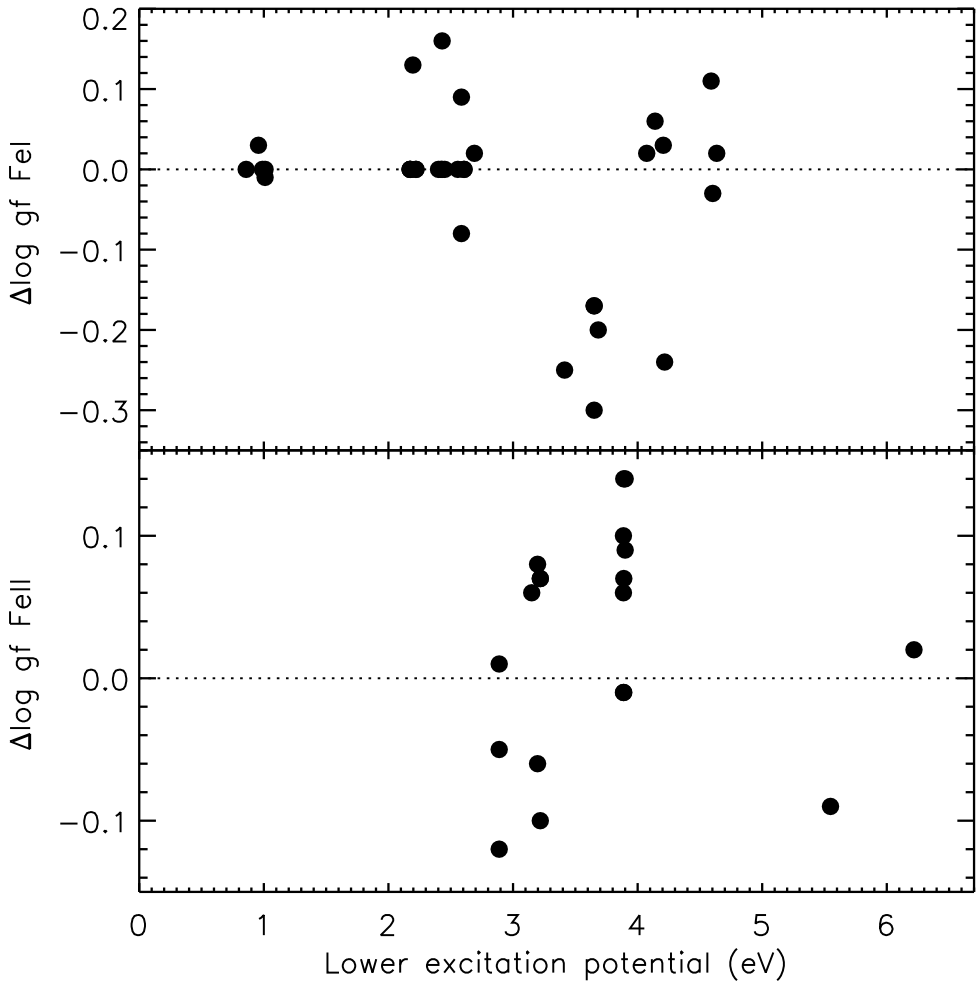

Fig. 5.— Comparison of the gf-values of Fe I (upper) and Fe II (lower) lines between this study and Fry & Carney (1997).

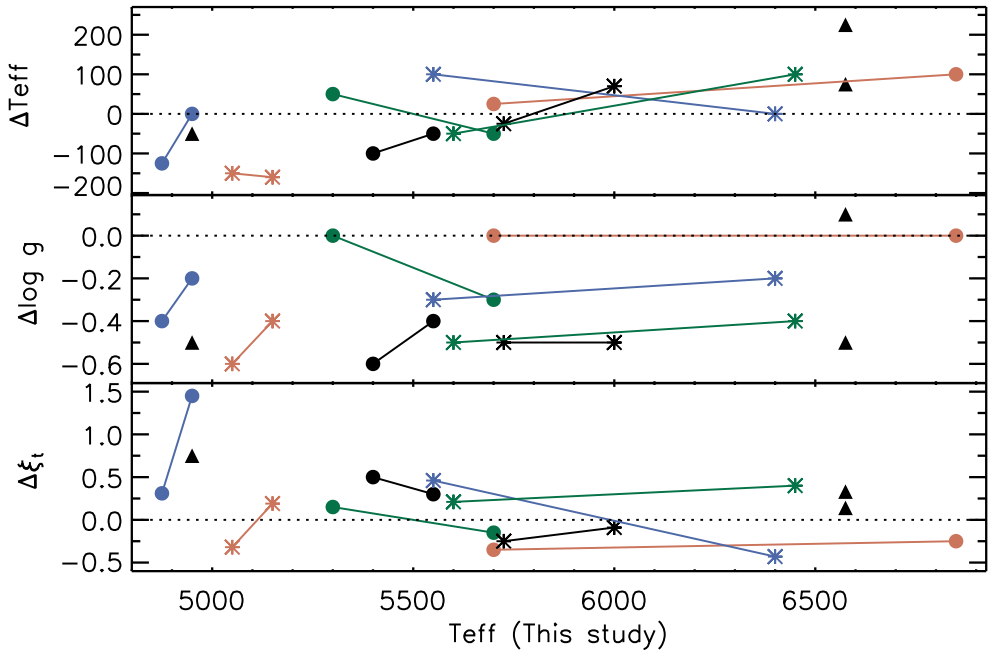

Fig. 6.— Stellar parameter differences for $T_{\rm eff}$, $\log g$, and ξ_t for THIS STUDY − FRY & CARNEY versus $T_{\rm eff}$ (this study). Solid lines connect the same Cepheids observed at different phases.

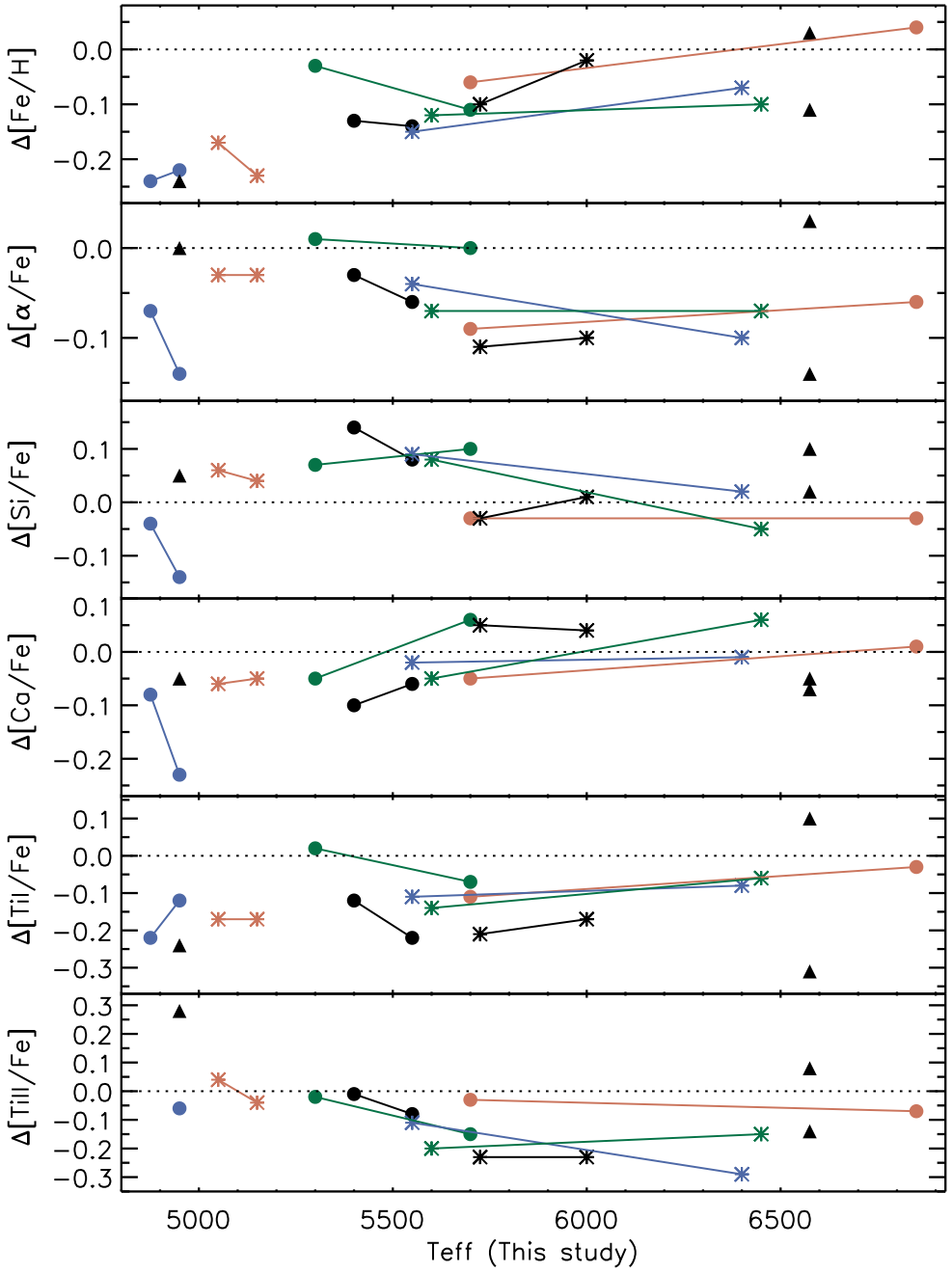

Fig. 7.— Abundance differences for [Fe/H] and [X/Fe] for THIS STUDY − FRY & CARNEY versus $T_{\rm eff}$ (this study). Solid lines connect the same Cepheids observed at different phases.

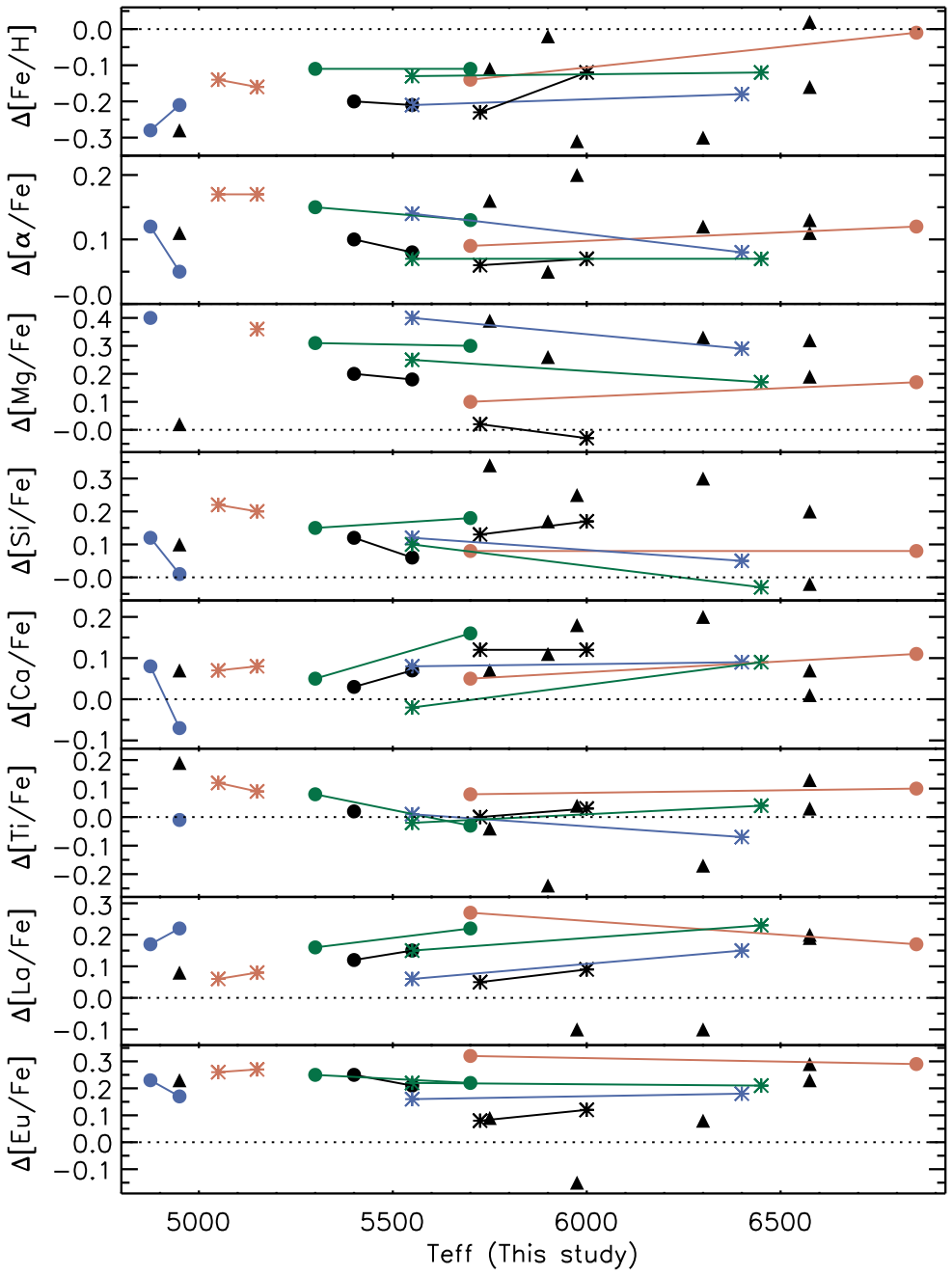

Fig. 8.— Abundance differences for [Fe/H] and [X/Fe] for THIS STUDY − ANDRIEVSKY versus $T_{\rm eff}$ (this study). Solid lines connect the same Cepheids observed at different phases.

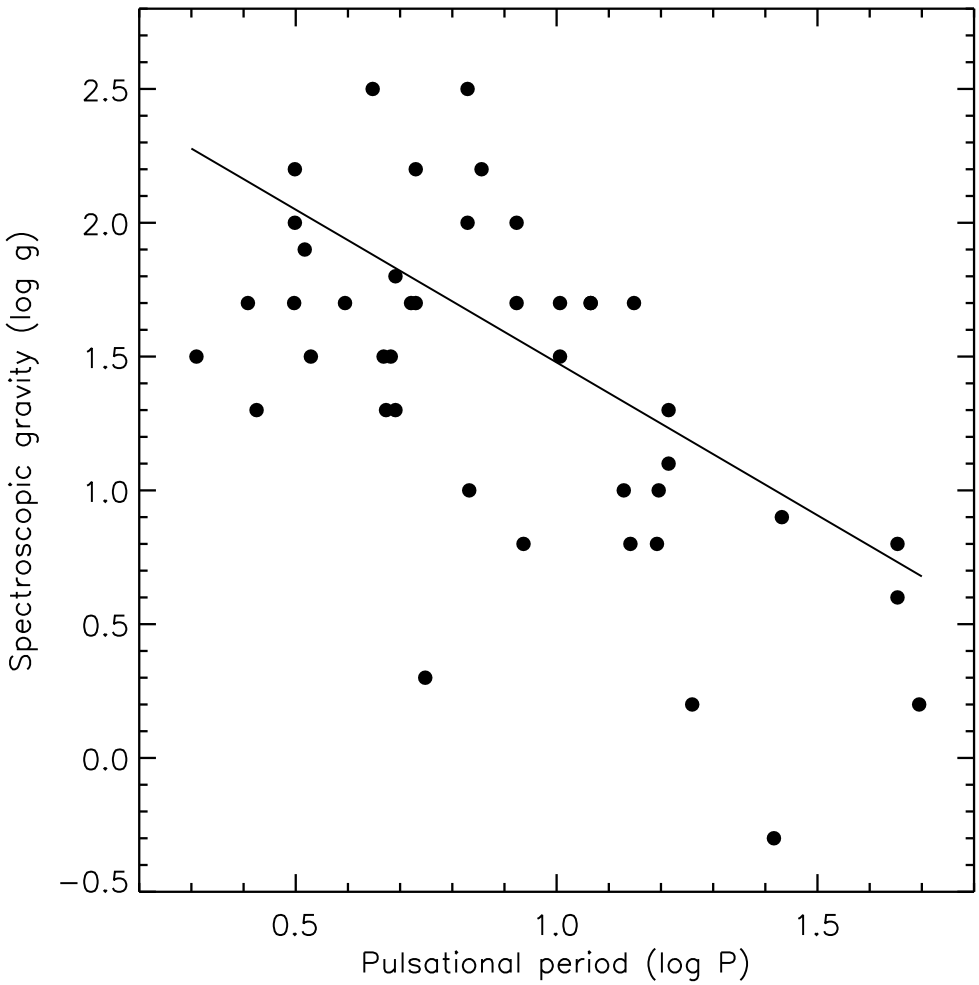

Fig. 9.— Spectroscopic gravities versus pulsational periods for the outer disk and comparison solar neighborhood Cepheids. The solid line is the period-gravity relation for radially pulsating variable stars defined by Fernie (1995).

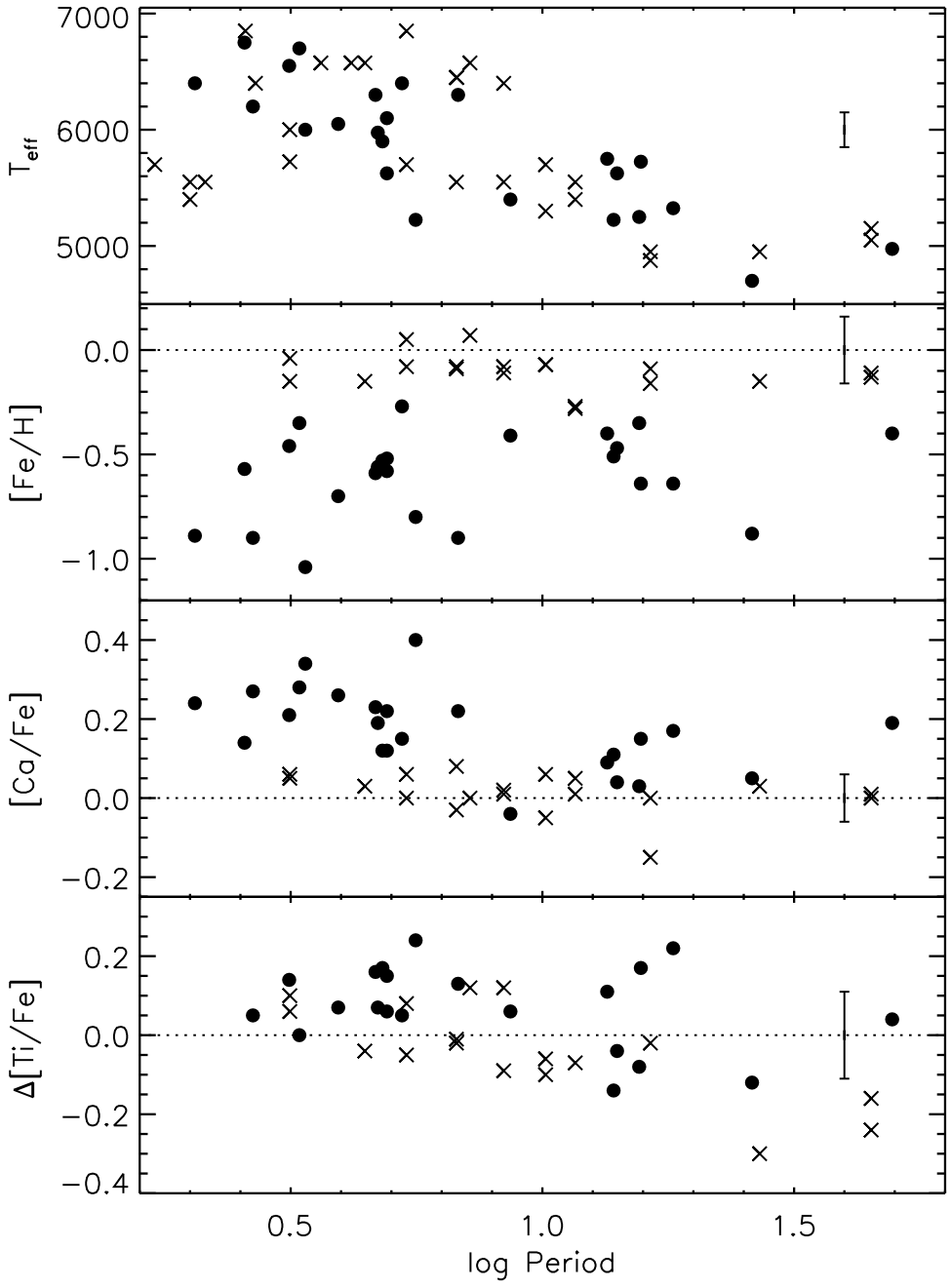

Fig. 10.— $T_{\rm eff}$ and abundance ratios versus period. The closed circles are our program Cepheids while the crosses represent the subset of Fry & Carney (1997) Cepheids re-analyzed in this study. A representative error bar is shown.

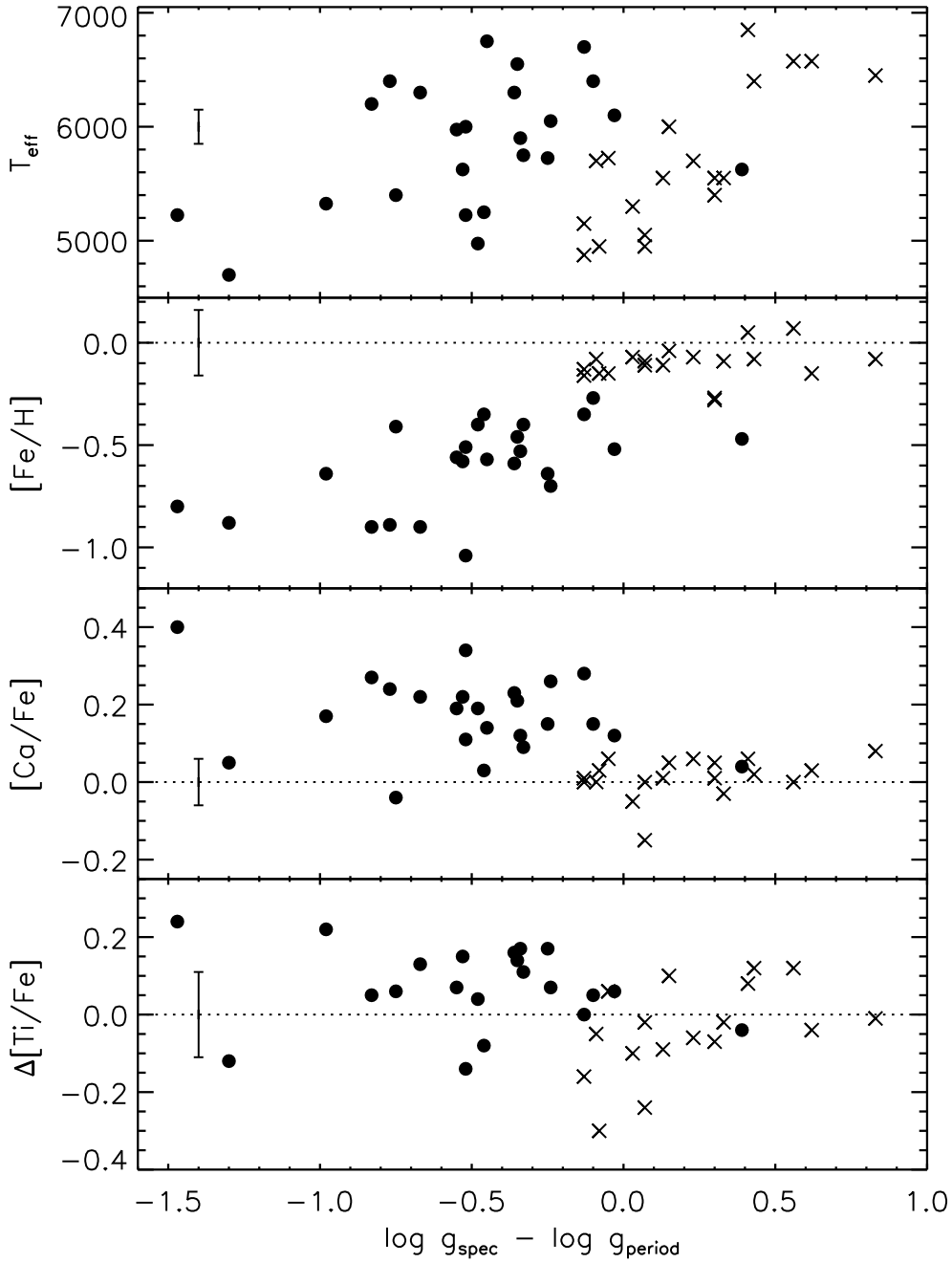

Fig. 11.— $T_{\rm eff}$ and abundance ratios versus the difference in surface gravity (spectroscopic − period [Fernie 1995]). The symbols are the same as in Figure 10.

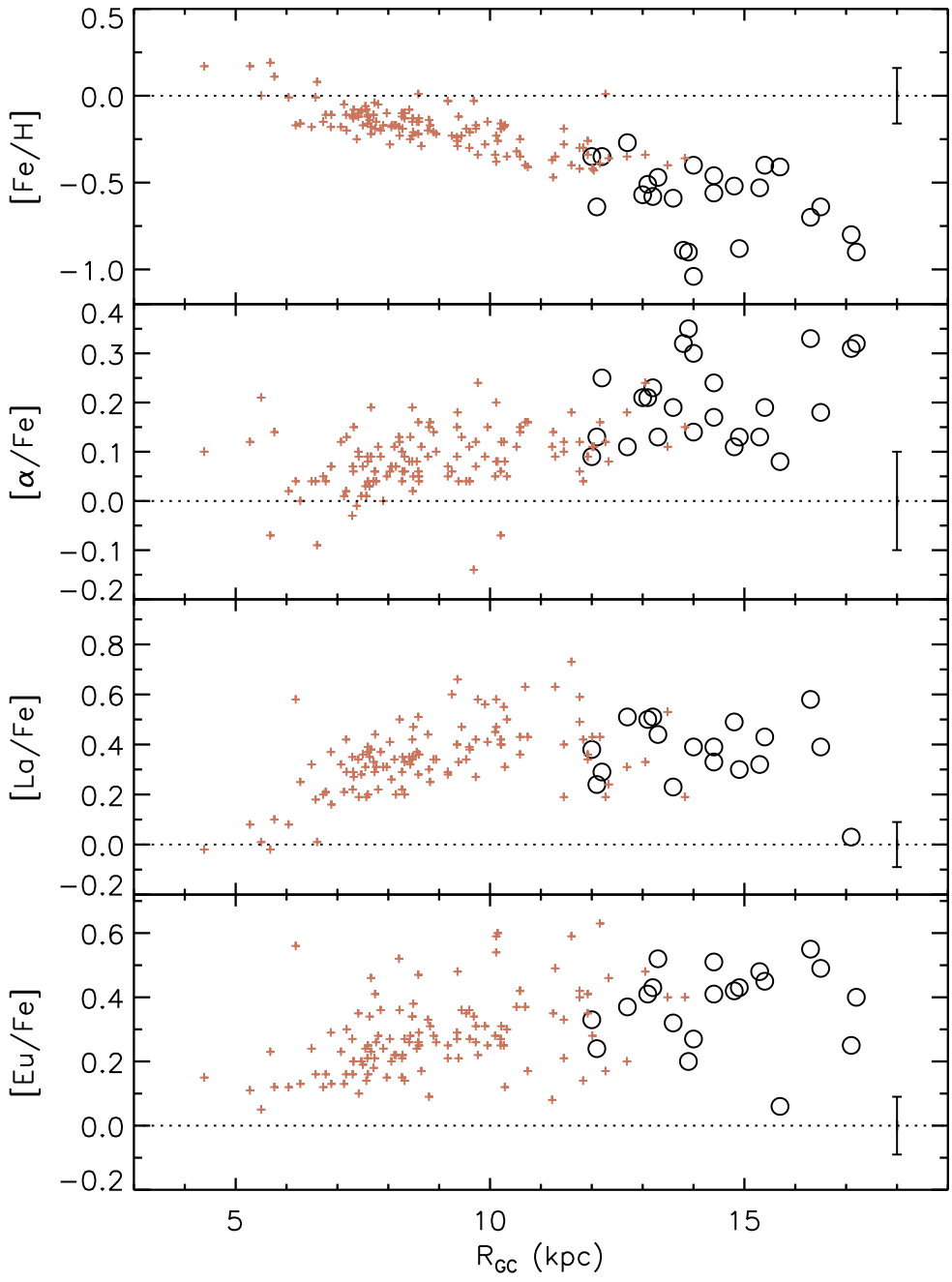

Fig. 12.— Abundance ratios [Fe/H], [α/Fe], [La/Fe], and [Eu/Fe] versus Galactocentric distance $R_{\rm GC}$ (kpc). The program Cepheids are represented by open black circles and the red plus signs are Cepheids from Andrievsky and collaborators. A representative error bar for the program Cepheids is shown.

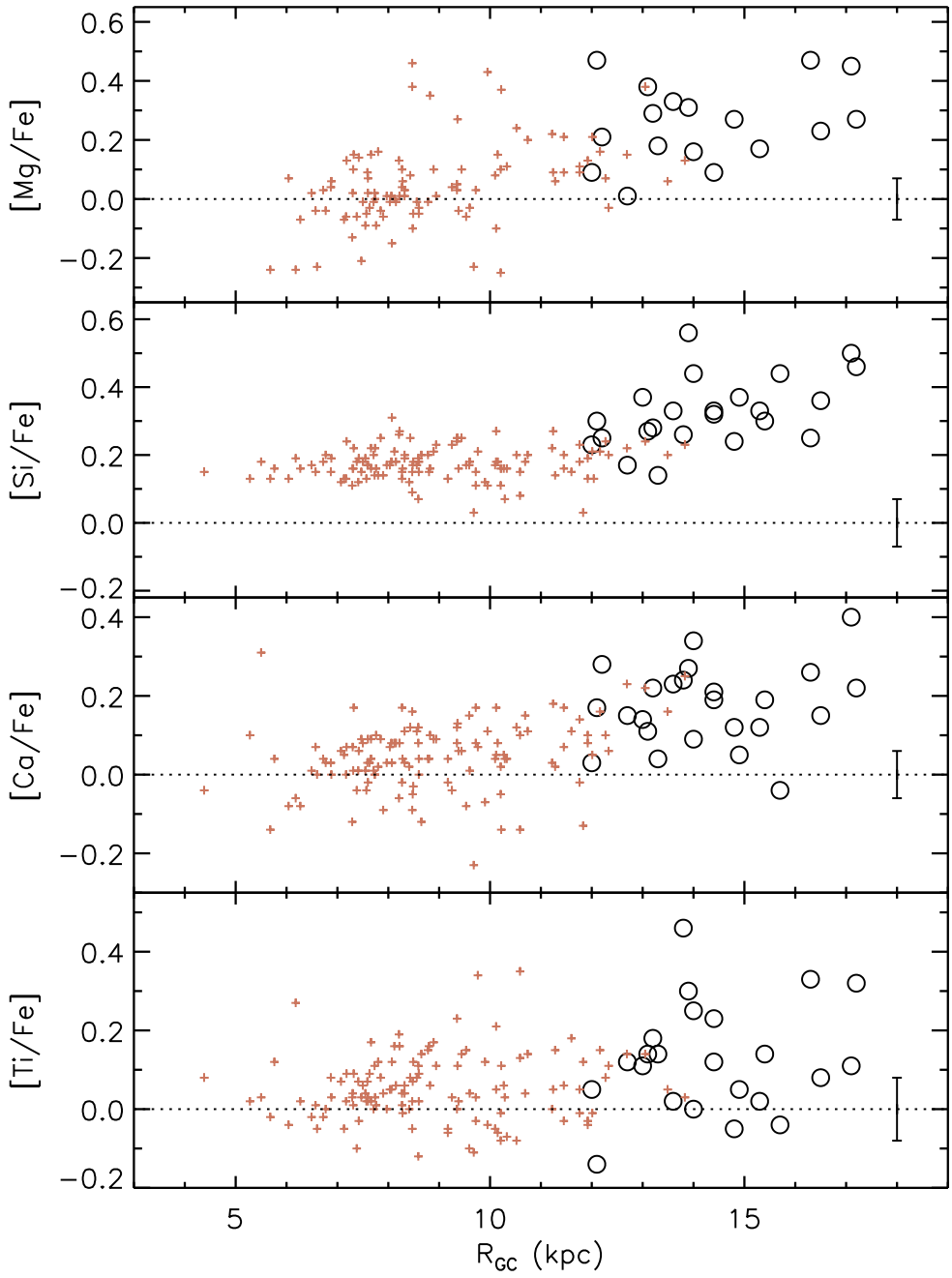

Fig. 13.— Abundance ratios [Mg/Fe], [Si/Fe], [Ca/Fe], and [Ti/Fe] versus Galactocentric distance $R_{\rm GC}$ (kpc). The symbols are the same as in Figure 12. A representative error bar for the program Cepheids is shown.

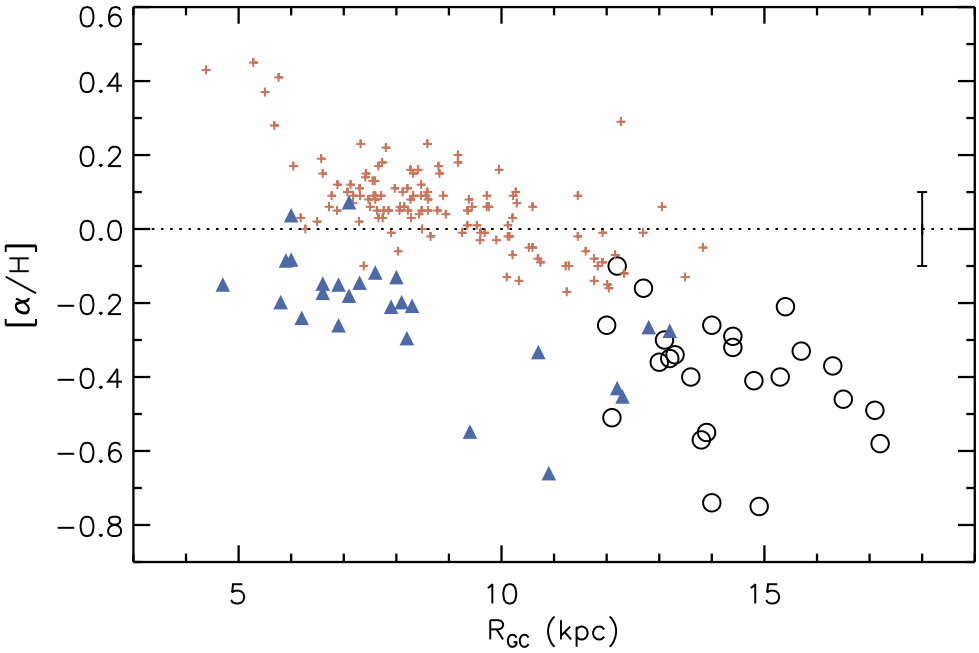

Fig. 14.— Abundance ratio [α/H] versus Galactocentric distance $R_{\rm GC}$ (kpc). The program Cepheids are represented by open black circles, the red plus signs are Cepheids from Andrievsky and collaborators, and the filled blue triangles are OB stars from Daflon & Cunha (2004). A representative error bar is shown.

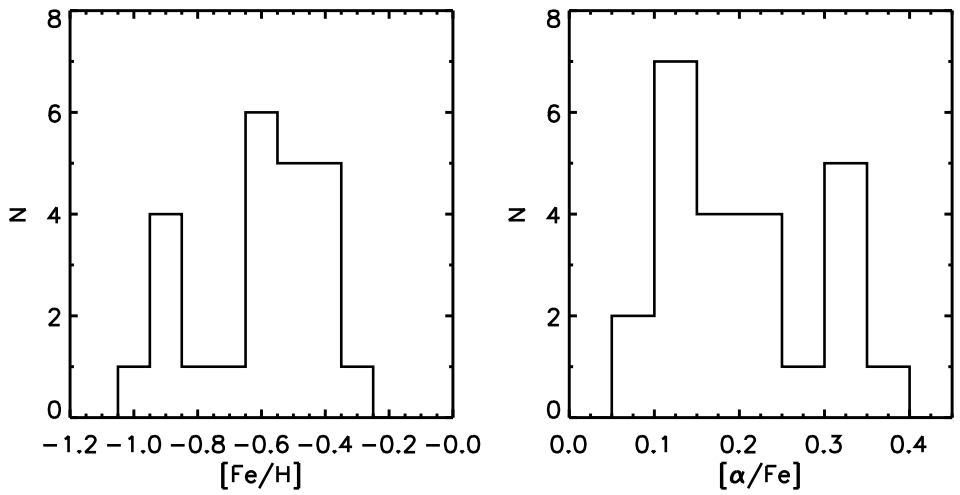

Fig. 15.— Metallicity distribution functions for [Fe/H] and [α/Fe].

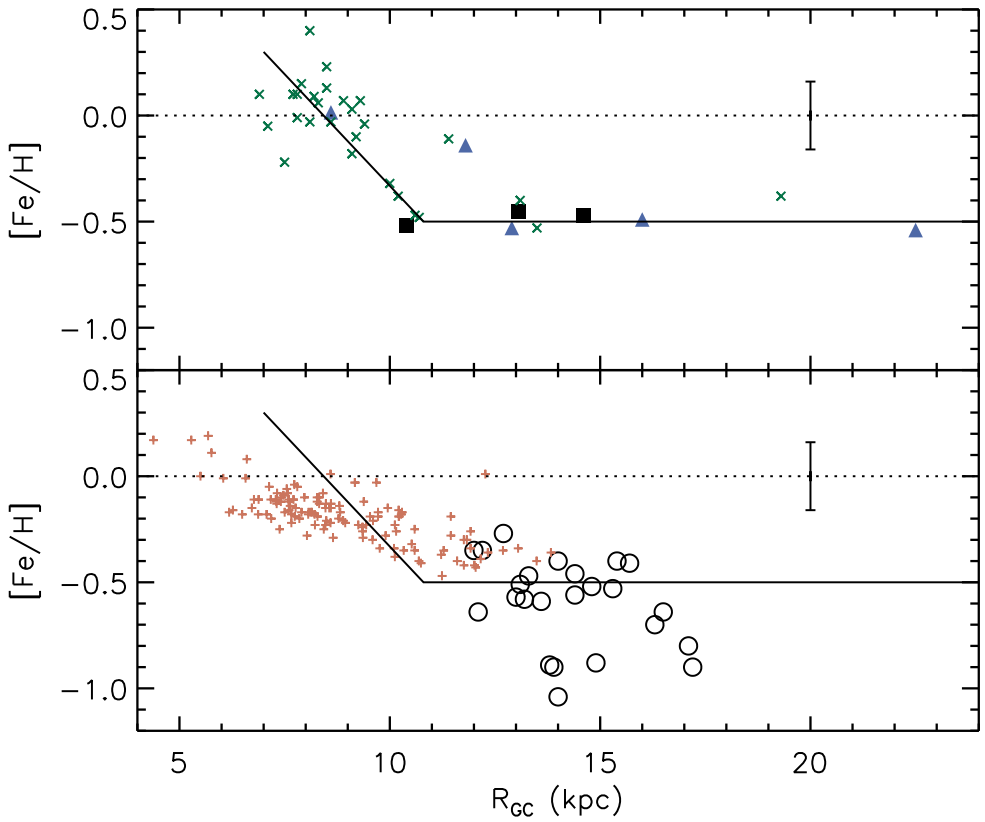

Fig. 16.— Abundance ratio [Fe/H] versus Galactocentric distance $R_{\rm GC}$ (kpc). In the upper panel, we plot the open cluster giants from Paper I (filled blue triangles), the field giants from Paper II (filled black squares), and open clusters (green crosses) from the compilation by Friel (2005). In the lower panel, we plot the program Cepheids (open black circles) and the Cepheids from Andrievsky and collaborators (red plus signs). In both panels, a representative error bar is shown. A schematic line fit to the data in the upper panel is shown in both panels.

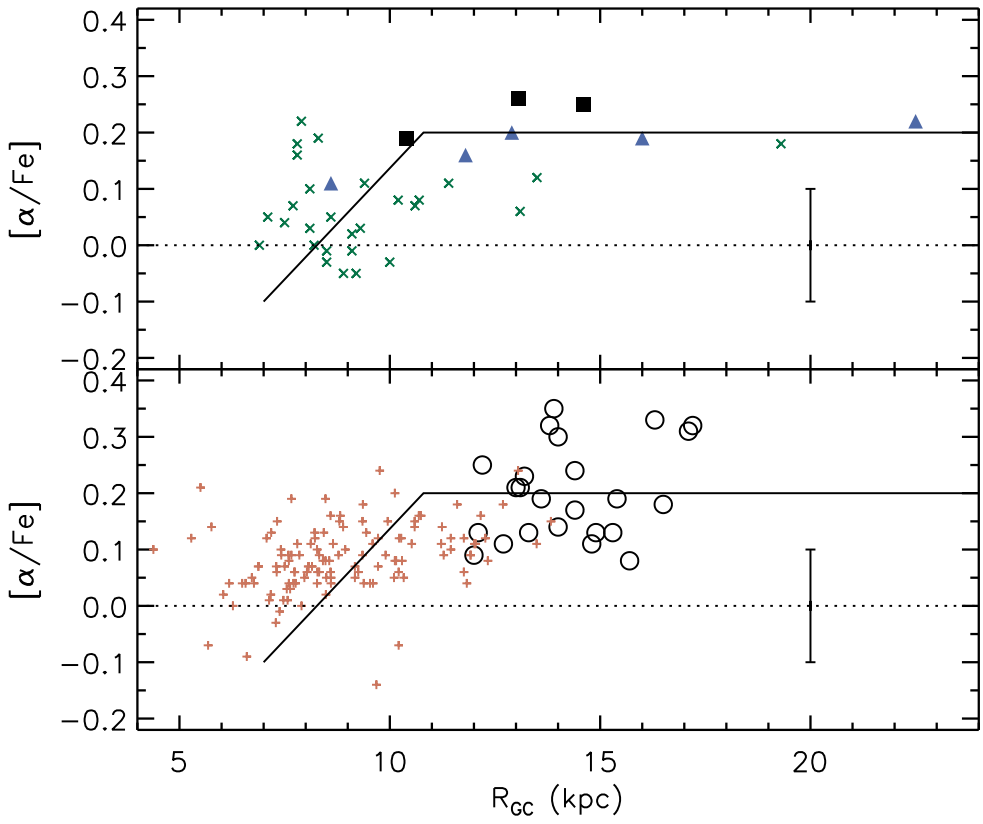

Fig. 17.— Same as Figure 16 but for the abundance ratio [α/Fe].

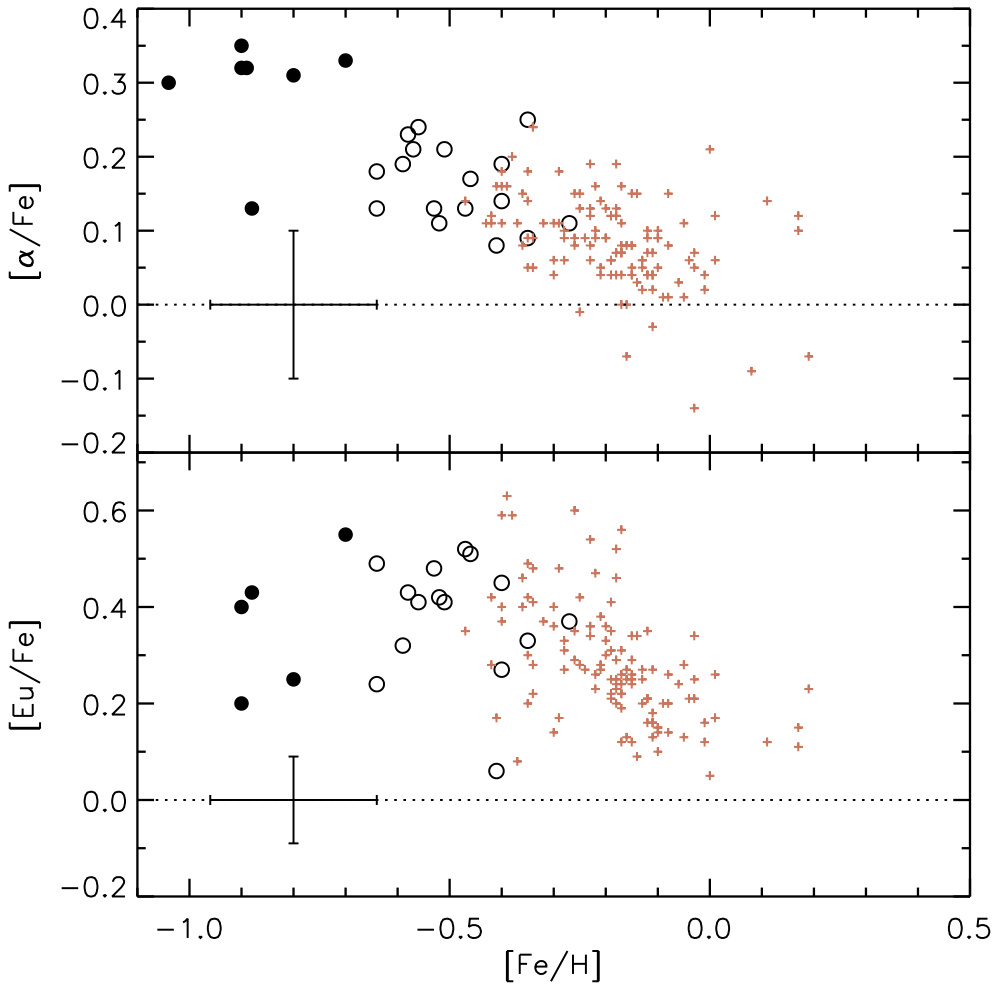

Fig. 18.— Abundance ratios [α/Fe] and [Eu/Fe] versus [Fe/H]. Open black circles are our "Galactic Cepheids", closed black circles are our "Merger Cepheids", and red plus signs are Andrievsky's Cepheids. A representative error bar for the program Cepheids is shown.

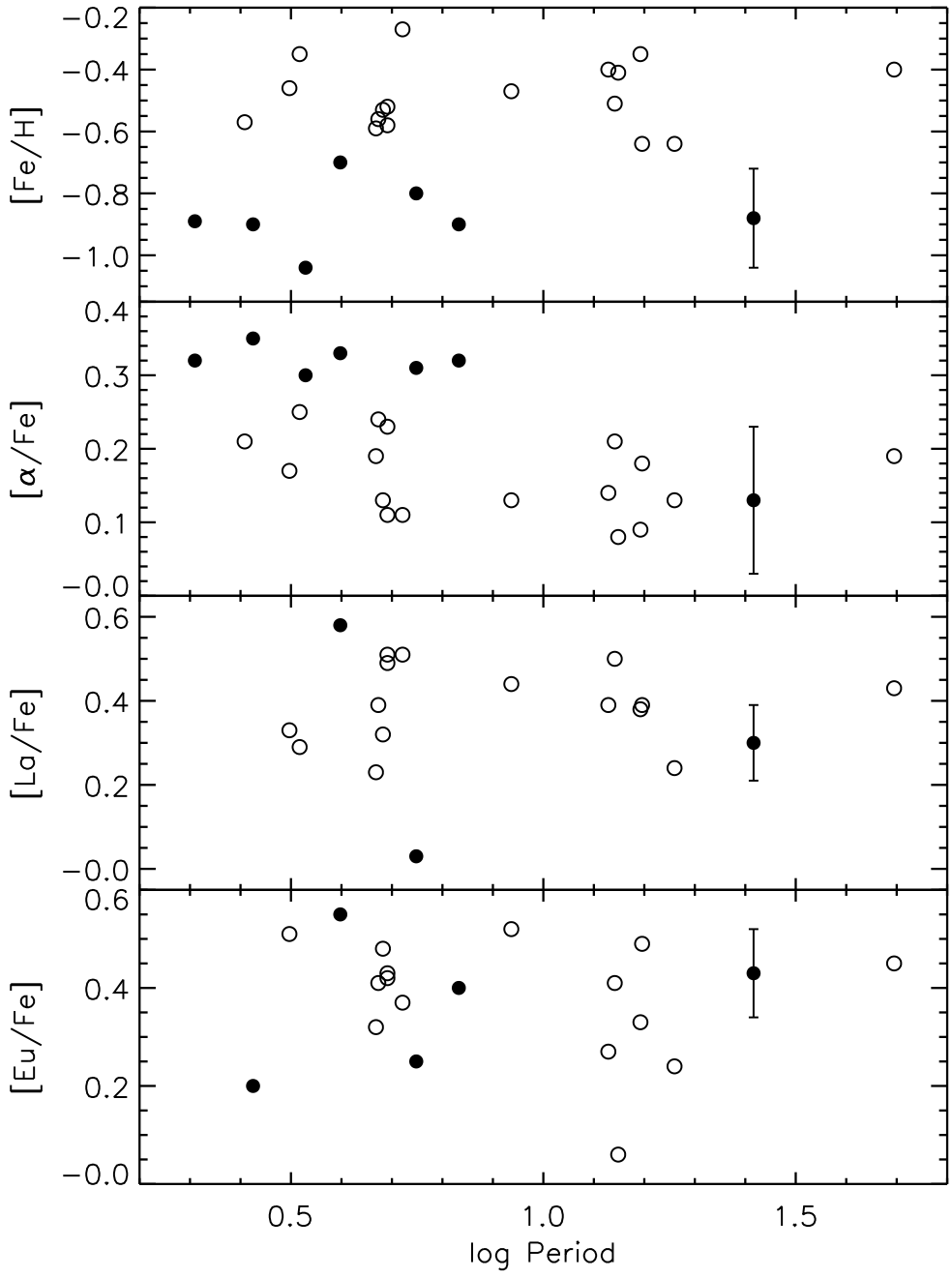

Fig. 19.— Abundance ratios [Fe/H], [α/Fe], [La/Fe], and [Eu/Fe] versus log Period. Open black circles are our "Galactic Cepheids" and closed black circles are our "Merger Cepheids". A representative error bar is shown.